JACS
JOURNAL OF THE AMERICAN CHEMICAL SOCIETY
pubs.acs.org/JACS
Article

Reductive C−C Coupling from Molecular Au(I) Hydrocarbyl Complexes: A Mechanistic Study

Juan Miranda-Pizarro,[§] Zhongwen Luo,[§] Juan J. Moreno, Diane A. Dickie, Jesús Campos,* and T. Brent Gunnoe*

Cite This: *J. Am. Chem. Soc.* 2021, 143, 2509−2522

Read Online

ACCESS | Metrics & More | Article Recommendations | Supporting Information

ABSTRACT: Organometallic gold complexes are used in a range of catalytic reactions, and they often serve as catalyst precursors that mediate C−C bond formation. In this study, we investigate C−C coupling to form ethane from various phosphine-ligated gem-digold(I) methyl complexes including $[Au_2(\mu\text{-}CH_3)(PMe_2Ar')_2][NTf_2]$, $[Au_2(\mu\text{-}CH_3)(XPhos)_2][NTf_2]$, and $[Au_2(\mu\text{-}CH_3)(^t\text{BuXPhos})_2][NTf_2]$ {Ar′ = C_6H_3-2,6-(C_6H_3-2,6-Me)$_2$, C_6H_3-2,6-(C_6H_2-2,4,6-Me)$_2$, C_6H_3-2,6-(C_6H_3-2,6-^{i}Pr)$_2$, or C_6H_3-2,6-(C_6H_2-2,4,6-^{i}Pr)$_2$; XPhos = 2-dicyclohexylphosphino-2′,4′,6′-triisopropylbiphenyl; ^{t}BuXPhos = 2-di-*tert*-butylphosphino-2′,4′,6′-triisopropylbiphenyl; NTf_2 = bis(trifluoromethyl sulfonylimide)}. The gem-digold methyl complexes are synthesized through reaction between $Au(CH_3)L$ and $Au(L)(NTf_2)$ {L = phosphines listed above}. For $[Au_2(\mu\text{-}CH_3)(XPhos)_2][NTf_2]$ and $[Au_2(\mu\text{-}CH_3)(^t\text{BuXPhos})_2][NTf_2]$, solid-state X-ray structures have been elucidated. The rate of ethane formation from $[Au_2(\mu\text{-}CH_3)(PMe_2Ar')_2][NTf_2]$ increases as the steric bulk of the phosphine substituent Ar′ decreases. Monitoring the rate of ethane elimination reactions by multinuclear NMR spectroscopy provides evidence for a second-order dependence on the gem-digold methyl complexes. Using experimental and computational evidence, it is proposed that the mechanism of C−C coupling likely involves (1) cleavage of $[Au_2(\mu\text{-}CH_3)(PMe_2Ar')_2][NTf_2]$ to form $Au(PR_2Ar')(NTf_2)$ and $Au(CH_3)(PMe_2Ar')$, (2) phosphine migration from a second equivalent of $[Au_2(\mu\text{-}CH_3)(PMe_2Ar')_2][NTf_2]$ aided by binding of the Lewis acidic $[Au(PMe_2Ar')]^+$, formed in step 1, to produce $[Au_2(CH_3)(PMe_2Ar')][NTf_2]$ and $[Au_2(PMe_2Ar')]^+$, and (3) recombination of $[Au_2(CH_3)(PMe_2Ar')][NTf_2]$ and $Au(CH_3)(PMe_2Ar')$ to eliminate ethane.

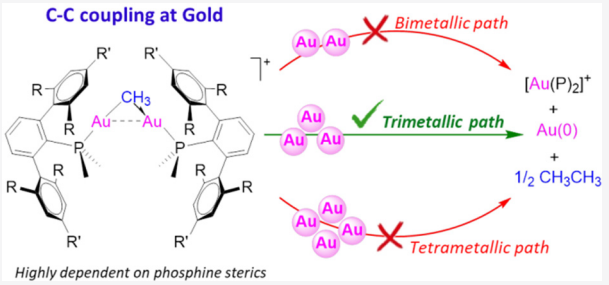

INTRODUCTION

Organometallic gold precatalysts have been applied to a range of catalytic organic syntheses.[1−9] Among the Au-catalyzed processes, many involve C−C bond forming reactions as a key step. Thus, the mechanisms of Au-mediated C−C bond formation have been of substantial interest.[10−20] Also, Au-catalyzed partial oxidation of methane in oleum to form methylbisulfate has been reported.[21,22] Demonstration, separately, of Au-mediated methane C−H activation[23,24] and of the ability of molecular Au complexes to mediate C−C bond forming reactions[14−22] sparked our interest in ethane elimination since combined methane C−H activation and ethane reductive elimination provides a strategy for the oxidative conversion of methane to ethane.[25,26] Herein, we disclose a mechanistic study of ethane elimination from phosphine-ligated gem-digold[27] methyl complexes with the general formula $[Au_2(\mu\text{-}CH_3)(PMe_2Ar')_2][NTf_2]$, $[Au_2(\mu\text{-}CH_3)(XPhos)_2][NTf_2]$, and $[Au_2(\mu\text{-}CH_3)(^t\text{BuXPhos})_2][NTf_2]$ {Ar = C_6H_3-2,6-(C_6H_3-2,6-Me)$_2$, C_6H_3-2,6-(C_6H_3-2,4,6-Me)$_2$, C_6H_3-2,6-(C_6H_3-2,6-^{i}Pr)$_2$, or C_6H_3-2,6-(C_6H_3-2,4,6-^{i}Pr)$_2$; XPhos = 2-dicyclohexylphosphino-2′,4′,6′-triisopropylbiphenyl; ^{t}BuXPhos = 2-di-*tert*-butylphosphino-2′,4′,6′-triisopropylbiphenyl; NTf_2 = bis(trifluoromethyl sulfonyl)-imide}.

Proposed mechanisms for Au-mediated C−C bond formation include reductive elimination from Au^{III} intermediates (Scheme 1).[28] For example, reductive elimination from $(R)_2Au(X)(L)$ (L = phosphine; R = Me, Et, or ^{n}Pr; X = anionic ligand such as Cl, OTf, NO_3, O_2CCF_3, or another alkyl ligand) was investigated by Kochi and co-workers, and reductive eliminations from $[(Me)_2Au(L)_2]^+$ complexes have been reported.[18,29,30] The proposed mechanism involves initial phosphine dissociation followed by C−C reductive elimination from the three-coordinate $R_2Au^{III}X$ intermediate (Scheme 1a). When R = Me, isotopic labeling studies with $(Me)_2AuX(L)$ and $(CD_3)_2Au(X)(L)$ (L = phosphine) indicate kinetically competitive intermolecular transfer of Me between two Au

Received: October 27, 2020
Published: February 5, 2021

https://dx.doi.org/10.1021/jacs.0c11296
J. Am. Chem. Soc. 2021, 143, 2509−2522

Scheme 1. Proposed Pathways of C−C Bond Coupling Reactions Mediated by Molecular Gold Complexes[17,18,31,36]

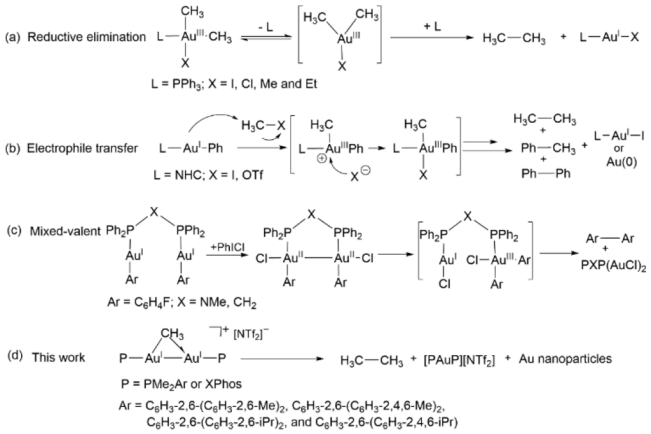

centers, but these alkyl transfers appear to occur only in nonpolar solvents.[23] Further, the putative binuclear Au intermediates responsible for alkyl transfer were not directly implicated in the C−C coupling reactions. From the starting complexes $(Me)_2Au(X)(L)$ (L = phosphine), it was proposed that larger phosphines facilitate ethane reductive elimination.[30] Alternatively, Kochi has proposed that ethane formation could result from digold alkyl intermediates, but to our knowledge, such reactions were not directly observed.[31,32] Other examples of ethane formation through bimolecular reductive elimination from $M-CH_3$ species include Ni^{II},[33] Cu^{I},[34] and Ru^{II}.[35]

The formation of C−C bonds from $(NHC)Au^{I}-R$ (NHC = *N*-heterocyclic carbene; R = Ph, Me, or *p*-tolyl) occurs upon addition of electrophiles (R′X), such as PhI, MeI, and MeOTf, to form R−R′ as well as homocoupled products R−R and R′−R′ (Scheme 1b).[36−38] The proposed mechanism involves formal *trans* oxidative addition of the electrophile (R′X) to form an $(NHC)Au^{III}(R')(X)(R)$ intermediate, followed by competitive (a) C−C reductive elimination to form R′−R and (b) intermolecular transfer of RX from a Au(III) intermediate to $(NHC)Au^{I}-R$ to yield $(NHC)Au^{III}(R)_2(X)$ followed by C−C reductive elimination to give the homocoupled product R−R. Related to these processes, the addition of F^{+}-donors to Au(I) hydrocarbyl compounds also promotes C−C coupling reactions.[39−42]

Mixed-valent gold hydrocarbyl complexes have also been proposed as intermediates responsible for the C—C bond formation.[17] For example, Toste and co-workers reported a fast biaryl C−C bond reductive elimination from a mixed-valent bimetallic Au^{I}/Au^{III} complex $[ClAu]PNP[AuCl(C_6H_4\text{-}4\text{-}F)_2]$ (PNP = $Ph_2P—N(CH_3)—PPh_2$) (Scheme 1c).[17] In this study, the Au(I) complex $[Au(C_6H_4\text{-}4\text{-}F)]PNP[Au(C_6H_4\text{-}4\text{-}F)]$ is oxidized with $PhICl_2$ to generate a symmetric bimetallic Au(II) species, $[ClAu(C_6H_4\text{-}4\text{-}F)]PNP[Au(C_6H_4\text{-}4\text{-}F)Cl]$. The latter isomerizes to a mixed-valent Au^{I}/Au^{III} complex, $[ClAu]PNP[AuCl(C_6H_4\text{-}4\text{-}F)_2]$, which undergoes reductive elimination to form a biaryl product. Similarly, O'Hair and co-workers reported a concerted redox couple mechanism from a reaction between allylic halides (CH_2 = $CHCH_2X$, X = Cl, Br, and I) and a gem-digold(I) compound, $[(dppm)_2Au_2Ph]^{+}$ (dppm = bis(diphenylphosphino)methane, $(Ph_2P)_2CH_2$).[43] It is hypothesized that the reductive coupling occurs from a Au^{I}/Au^{III} complex, $[ClAu^{I}](dppm)[Au^{III}(CH_2{=}CHCH_2)(Ph)]$.

Germane to these proposed binuclear Au precursors to C—C elimination, several gem-digold intermediates have been reported, including $[Au_2(\sigma,\pi\text{-}CH{=}CHC_3H_5)(PPh_3)_2][NTf_2]$,[44] $[Au_2(\mu\text{-}Ph)L_2][NTf_2]$[45] (L = PPh_3 or NHC), and $[Au_2(\mu\text{-}R)(PMe_2Ar^{Dipp2})_2][NTf_2]$ (R = CH_3, $CH{=}CH_2$, $C{\equiv}CH$, $Ar^{Dipp2}{=}C_6H_3\text{-}2,6\text{-}(C_6H_3\text{-}2,6\text{-}{}^{i}Pr)_2$).[46] The thermal stabilities of phosphine-ligated gem-digold hydrocarbyl complexes have been reported to depend on the steric properties of the ancillary ligands.[46] Other related examples, including $[Au_2(\mu\text{-}vinyl^{cypr})(PPh_3)_2][NTf_2]$[14,15,44] and $[Au_2(\mu\text{-}vinyl^{cypr})(PPh_3)_2][NTf_2]$, readily decompose to the corresponding diene, $[Au(PPh_3)_2][NTf_2]$, and colloidal gold byproducts. Nonetheless, a mechanistic understanding of these C—C coupling processes and, in general, of C—C formation from Au^{I} complexes is lacking.

Herein, we explore the formation of ethane from one of the simplest possible gold-based systems, namely, $Au(CH_3)(PPh_3)$. To enable reliable mechanistic investigations, we extended our preliminary observations on triphenylphosphine-ligated systems to bulkier terphenyl and biaryl phosphines that provide kinetic stabilization of key digold intermediates. In particular, we have focused on C−C coupling reactions from gem-digold methyl complexes with a general formula $[Au_2(\mu\text{-}CH_3)(PMe_2Ar')_2][NTf_2]$ and $[Au_2(\mu\text{-}CH_3)(XPhos)_2][NTf_2]$ (Figure 1). We studied the impact of the phosphine ligand on the stability of digold complexes, especially the influence on ethane elimination.

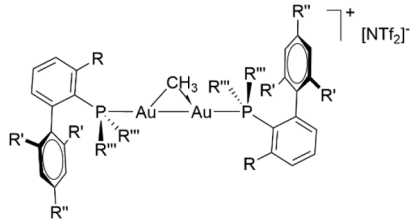

4a, R = Xyl; R′ = Me; R″ = H; R‴ = Me, **4d**, R = Trip; R′ = iPr; R″ = iPr; R‴ = Me
4b, R = Mes; R′ = Me; R″ = Me; R‴ = Me, **4e**, R = H; R′ = iPr; R″ = iPr; R‴ = Cy
4c, R = Dipp; R′ = iPr; R″ = H; R‴ = Me, **4f**, R = H; R′ = iPr; R″ = iPr; R‴ = tBu

Figure 1. Phosphine-ligated gem-digold methyl complexes with the general formula $[Au_2(\mu\text{-}CH_3)(PR_2Ar')_2][NTf_2]$ investigated in this work (Xyl = 2,6-C_6H_3-Me_2; Mes = 2,4,6-C_6H_2-Me_3; Dipp = 2,6-C_6H_3-$^{i}Pr_2$; Tripp = 2,4,6-C_6H_2-$^{i}Pr_3$).

RESULTS AND DISCUSSION

Synthesis of Neutral Gold Complexes Based on Terphenyl and Biaryl Phosphines. Gold complexes with terphenyl phosphine (complexes **1a**−**1d** in Scheme 2) and with biaryl "Buchwald phosphine" ligands (**1e** and **1f**) were synthesized by methylation of Au(I) chloride precursors with MeMgX (X = Cl or Br) in 60−80% isolated yields.[47] Formation of the new Au−C bonds is evidenced by the appearance of ^{1}H NMR resonances in the range from 0.08 to 0.45 ppm with associated $^{13}C\{^{1}H\}$ signals at 3.4 to 8.3 ppm ($^{2}J_{CP} \approx 100$ Hz). Single crystals of **1a**, **1e**, and **1f** were obtained by slow evaporation from a mixture of pentane and diethyl ether or pentane and dichloromethane solution from 5 to −25 °C (Figure 2). The solid-state structures of complexes **1e** and **1f** show a weak κ^{1} type interaction (localized Au···π(arene) contact)[48−50] between the Au(I) center and the *ipso* carbon of the arenes (C20, **1e**; C16, **1f**) with bond distances of 3.1748(17) and 3.180(4) Å, respectively. The distances

https://dx.doi.org/10.1021/jacs.0c11296
J. Am. Chem. Soc. 2021, 143, 2509−2522

Scheme 2. Synthesis of Phosphine-Ligated Gold Methyl Compounds with Terphenyl Phosphines (1a−1d) and Buchwald Phosphines (1e and 1f)

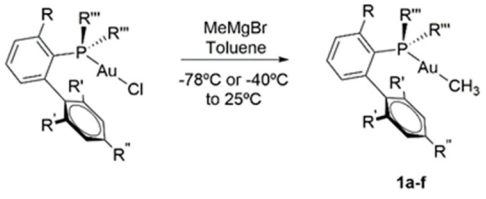

1a, R = Xyl; R' = Me; R'' = H; R''' = Me, **1d**, R = Trip; R' = iPr; R'' = iPr; R''' = Me
1b, R = Mes; R' = Me; R'' = Me; R''' = Me, **1e**, R = H; R' = iPr; R'' = iPr; R''' = Cy
1c, R = Dipp; R' = iPr; R'' = H; R''' = Me, **1f**, R = H; R' = iPr; R'' = iPr; R''' = tBu

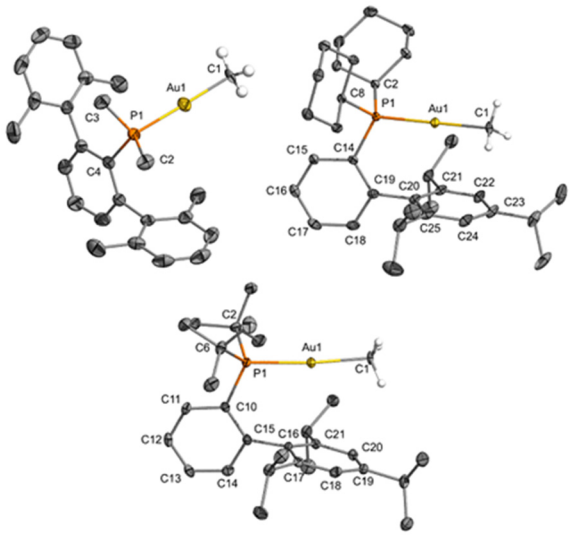

Figure 2. ORTEPs of $Au(CH_3)(PMe_2Ar^{Xyl2})$ (**1a**), $Au(CH_3)$-(XPhos)(**1e**), and $Au(CH_3)(^tBuXPhos)$ (**1f**) represented at 50% probability. (For **1f**, one of the two chemically equivalent, but crystallographically distinct, structures is shown. For the second structure, see the Supporting Information.) Hydrogen atoms on the phosphine ligands are omitted for clarity. Selected bond lengths (Å): **1a**, Au1−C1 = 2.123(2); P1−C2 = 1.825(3); P1−C3 = 1.823(3); P1−C4 = 1.852(2); Au1−P1 = 2.2900(7). **1e**, Au1−C1 = 2.1146(14); Au1−C20 = 3.1748(17); Au1−C25 = 3.2510(18); Au1−C21 = 3.5023(18); Au−arene (arene ring centroid) = 3.2659(10); Au1−P1 = 2.2917(4). **1f**, Au1−C1 = 2.096(4); Au1−C16 = 3.180(4); Au1−C17 = 3.551(4); Au1−C21 = 3.409(4); Au−arene (benzene ring centroid) = 3.449(2); Au1−P1 = 2.3007(11). Selected bond angles (deg): **1a**, P1−Au1−C1 = 178.97(8); C2−P1−Au1 = 112.8(1); C3−P1−Au1 = 111.95(10); C4−P1−Au1 = 113.14(8). **1e**, P1−Au1−C1 = 179.57(4); C14−P1−Au1 = 117.53(5). **1f**, C1−Au1−P1 = 172.80(12); C10−P1−Au1 = 115.25(13).

between Au centers and arene ring centroids are 3.2659(10) Å (**1e**) and 3.449(2) Å (**1f**), also indicative of intramolecular Au···π(arene) interactions.[50,51] Structure **1a** does not exhibit this type of contact, in agreement with the preferred geometry adopted by the smaller phosphines of the terphenyl series.[52] The Au−CH_3 bond distances are 2.123(2) Å (**1a**), 2.1146(14) Å (**1e**), and 2.096(4) Å (**1f**).

Terminal ethyl and phenyl complexes $Au(C_2H_5)$-(PMe_2Ar^{Xyl2}) (**2a**) and $Au(C_6H_5)(PMe_2Ar^{Xyl2})$ (**3a**) were synthesized with the aim of exploring the possibility of C−C bond heterocoupling with different hydrocarbyl substituents bound to gold (see below). These compounds were prepared by a similar procedure to their methyl analogues and characterized by spectroscopic techniques and single-crystal X-ray diffraction (Figures 3 and 4). The σ Au−C bond

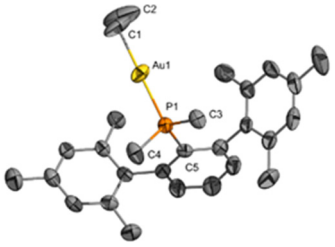

Figure 3. ORTEP of $Au(C_2H_5)(PMe_2Ar^{Mes2})$ (**2a**) at 50% probability (one of the two crystallographically distinct structures, the other one being $Au(C_2H_5)(PMe_2Ar^{Xyl2})$, see Figure S1). Hydrogen atoms on the phosphine ligands are omitted for clarity. Selected bond lengths (Å): Au1−C1 = 2.079(8); C1−C2 = 1.411(15). Selected bond angles (deg): C1−Au1−P1 = 179.6(3); Au1−C1−C2 = 115.0(7); C3−P1−Au1 = 111.5(3); C5−P1−Au1 = 115.63(19); C4−P1−Au1 = 112.2(3).

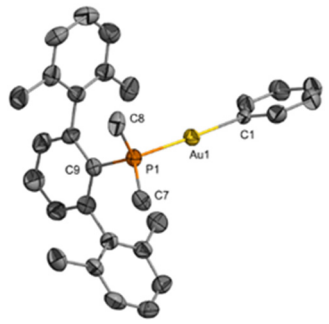

Figure 4. ORTEP of $Au(C_6H_5)(PMe_2Ar^{Xyl2})$ (**3a**) at 50% probability. Hydrogen atoms on the phosphine ligands are omitted for clarity. Selected bond lengths(Å): Au1−C1 = 2.089(7); Au1−P1 = 2.302(2). Selected bond angles (deg): C1−Au1−P1 = 177.7(2); C8−P1−Au1 = 110.4(3); C7−P1−Au1 = 109.9(3); C9−P1−Au1 = 117.5(2).

distances are 2.079(8) Å (**2a**) and 2.087(7) (**3a**) Å, which are similar to neutral Au−CH_3 bond distances discussed above. Complex **2a** cocrystallizes in a 1:1 ratio with a molecule of $Au(C_2H_5)(PMe_2Ar^{Mes2})$ (**2b**, see Figure S1), whose geometric parameters are comparable to those of **2a**. This is due to the fact that the crystals were obtained from a phosphine exchange experiment between **2a** and free PMe_2Ar^{Mes2} that was conducted as part of our mechanistic investigations (see below, Figure S1). The bond distance between C1 and C2 in the Au-ethyl fragment of **2a** is 1.411(15) Å, lying between the carbon−carbon lengths of ethylene (1.34 Å) and ethane (1.54 Å). The electrophilic nature of gold may enhance the C−C bond strength and thus shorten bond length compared to a typical C−C single bond. The structure of complex **3a** is similar to those of compounds **1** and **2a** and does not require further discussion.

Ethane Elimination from $Au(CH_3)(PPh_3)$. For the sake of simplicity and considering the widespread utilization of PPh_3-based gold complexes, we commenced our studies by exploring ethane elimination from $Au(CH_3)(PPh_3)$. This compound is stable at moderate temperatures as heating at 40 °C caused no apparent alteration when monitoring by ^1H and $^{31}P\{^1H\}$ NMR spectroscopy, and no ethane formation was detected. However, in the presence of 1 equiv of $Au(PPh_3)(NTf_2)$, $Au(CH_3)$-

https://dx.doi.org/10.1021/jacs.0c11296
J. Am. Chem. Soc. 2021, 143, 2509−2522

(PPh_3) evolves ethane immediately at room temperature with complete consumption of $Au(CH_3)(PPh_3)$ by the time of placing the sample in the NMR probe (<10 min; Scheme 3).

Scheme 3. Ethane Elimination from $Au(CH_3)(PPh_3)$ in the Presence of 1 equiv of $Au(PPh_3)(NTf_2)$

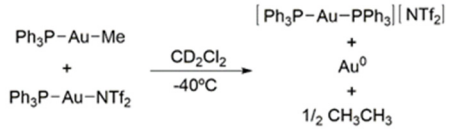

The release of ethane is accompanied by clean formation of the homoleptic bisphosphine complex $[Au(PPh_3)_2][NTf_2]$, along with Au(0), as evinced by the formation of black insoluble material. The nature of this solid was interrogated by transmission electron microscopy (TEM) analysis (Figure 5).

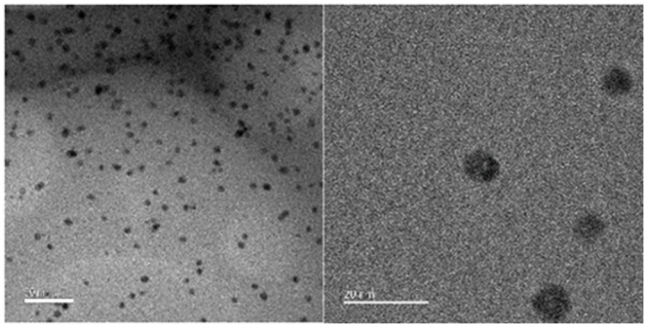

Figure 5. Transmission electron microscopy (TEM) analysis of the insoluble Au^0 particles produced during ethane evolution in Scheme 3.

When a 1:1 molar mixture of $Au(PPh_3)(NTf_2)$ and $Au(CH_3)(PPh_3)$ was dissolved in dichloromethane at −70 °C, ethane formation was detected immediately by ^1H NMR spectroscopy (Figure S9). Variable temperature ^1H and $^{31}P\{^1H\}$ NMR analysis from −70 to 25 °C revealed the formation of an intermediate species characterized by a broad ^1H NMR resonance at 1.6 ppm associated with a $^{31}P\{^1H\}$ NMR resonance at 37.5 ppm, which we attribute to the corresponding gem-digold methyl species $[Au_2(\mu\text{-}CH_3)(PPh_3)_2][NTf_2]$ (Figure S8).[46] However, this compound is only detectable at temperatures below −40 °C, and it rapidly evolves to the final products above this temperature.

Though the transient nature of $[Au_2(\mu\text{-}CH_3)(PPh_3)_2][NTf_2]$ prevented us from exploring its role in further detail, our initial kinetic investigations using 1 equiv of the related $Au(PPh_3)(NO_3)$ revealed a second-order dependence on neutral $Au(CH_3)(PPh_3)$ for ethane elimination (Figure S6). Nonetheless, we could carry out these studies with related methyl complexes based on biaryl and terphenyl phosphines, as discussed in the following sections. Since we observed the formation of gold nanoparticles during ethane elimination, we decided to probe for a possible catalytic role of Au nanoparticles in the C−C coupling reaction, particularly considering their catalytic role in related processes.[53−55] However, using independently prepared gold nanoparticles (i.e., Au/TiO_2 and Au/Fe_2O_3) as catalysts did not promote methyl C−C coupling at a comparable rate ($t_{1/2} \approx 1$ day at 25 °C). Thus, it seems unlikely that Au nanoparticles play a catalytic role in the formation of ethane. In addition, we tested for the possibility of a radical-mediated pathway. To do so, we combined equimolar amounts of $Au(CH_3)(PPh_3)$ and $[Au(PPh_3)][NTf_2]$ in the presence of excess toluene (10 equiv) as a radical probe. Under these conditions, the formation of $CH_3\bullet$ radicals should be quenched by toluene by means of hydrogen atom abstraction from the benzylic position.[56] This process would have released methane, which was not observed during our experiments, thus favoring the likelihood of a nonradical route.

Synthesis of Cationic gem-Digold Methyl Complexes. To probe if gem-digold methyl complexes are relevant intermediates during C−C coupling reactions, bulky terphenyl and Buchwald phosphines were used. Some of us have recently demonstrated that gem-digold methyl species are kinetically stabilized by large phosphine substituents,[46] which should facilitate kinetic investigations. Indeed, using the aforementioned bulky phosphines enabled the isolation and characterization of various uncommon gem-digold methyl complexes of type $[Au_2(\mu\text{-}CH_3)(PMe_2Ar')_2][NTf_2]$ (**4a−4d**). These were synthesized in high yields by mixing a 1:1 molar ratio of a Au(I) methyl complex $Au(CH_3)(PMe_2Ar')$ and the corresponding Au(I) bis(trifluoromethyl sulfonyl)imide (Scheme 4). Alternatively, the addition of 0.5 equiv of $[Ph_3C][B(C_6F_5)_4]$ to neutral Au(I) methyl complexes $Au(CH_3)(PR_2Ar')$ leads to the same gem-digold species in comparable yields.

Scheme 4. General Synthesis of the gem-Digold Methyl Complexes with Terphenyl Phosphines (4a−4d) and Buchwald Phosphine-Ligated gem-Digold Methyl Complexes (4e and 4f)

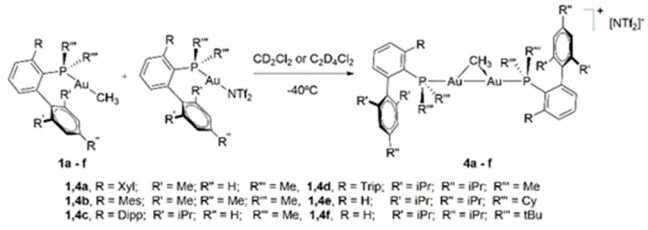

Compounds **4a−4f** were characterized by multinuclear NMR spectroscopy, and their purity was confirmed by microanalysis. Distinctive ^1H NMR signals due to the methyl group, which are slightly shifted to higher frequencies (ca. 0.5−1.2 ppm) compared to their corresponding neutral precursors (**1a−1f**), are consistent with the formation of the gem-digold complexes. The presence of the bridging methyl ligand is further confirmed by $^{13}C\{^1H\}$ NMR resonances shifted to lower frequencies by approximately 5 ppm compared to the parent compounds **1a−1f** and characterized by a drastically reduced scalar-coupling to ^{31}P (ca. 50 Hz; cf. ∼100 Hz for **1a−1f**). The compounds $[Au_2(\mu\text{-}CH_3)(XPhos)_2][NTf_2]$ (**4e**) and $[(Au)_2(\mu\text{-}CH_3)(^tBuXPhos)_2][NTf_2]$ (**4f**) were additionally authenticated by single-crystal X-ray diffraction (Figure 6; Table 1). The gold methyl bond distances in **4e** and **4f** are ∼0.1 Å longer than in their corresponding neutral methyl complexes **1e** and **1f**. A characteristic Au−arene interaction is discernible for the two structures. While the structure of **4f** exhibits a slightly shortened Au−arene distance (3.390(3) Å on average) than its neutral complex **1f** (3.449(2) Å), compound **4e** (3.432(2) Å on average) presents an apparently weaker Au−arene interaction than its neutral gold compound

https://dx.doi.org/10.1021/jacs.0c11296
J. Am. Chem. Soc. 2021, 143, 2509−2522

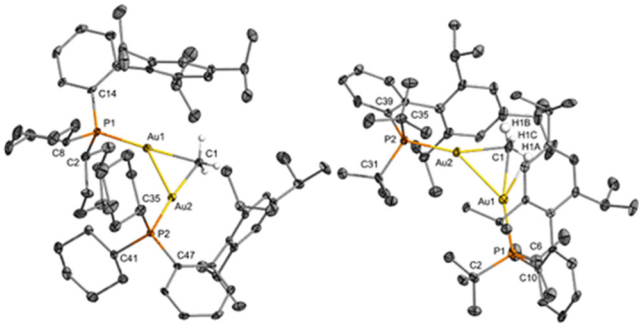

Figure 6. ORTEPs of $[Au_2(\mu\text{-}CH_3)(XPhos)_2][NTf_2]$ (**4e**) and $[(Au)_2(\mu\text{-}CH_3)(^tBuXPhos)_2][NTf_2]$ (**4f**) at 50% probability (for **4e**, only one of the three chemically equivalent, but crystallographically distinct, structures is represented). Hydrogen atoms on the phosphine ligands are omitted for clarity. Selected bond lengths (Å): **4e**, Au1−C1 = 2.221(5); Au2−C1 = 2.235(5); Au1−Au2 = 2.7466(4); Au1−P1 = 2.2637(12); Au2−P2 = 2.2662(13). **4f**, Au1−C1 = 2.204(9); Au2−C1 = 2.207(8); Au1−Au2 = 2.7763(7); Au1−P1 = 2.285(2); Au1−P2 = 2.2798(18). Selected bond angles (deg): **4e**, C1−Au1−P1 = 168.41(14); C1−Au2−P2 = 172.39(13); Au1−C1−Au2 = 76.11(16); C1−Au1−Au2 = 52.17(13); C1−Au2−Au1 = 51.72(12). **4f**, C1−Au1−P1 = 162.9(2); C1−Au2−P2 = 160.9(2); Au1−C1−Au2 = 78.0(3); C1−Au1−Au2 = 51.0 (2); C1−Au2−Au1 = 50.9 (2).

1e (3.2659(1) Å). The presence of intense aurophilic interactions[57,58] is evinced by Au···Au distances in complexes **4e** and **4f** of 2.7466(6) and 2.7763(7) Å, respectively. These Au···Au distances are slightly longer than those reported for the related **4c** (2.7120(8) Å) and ∼0.1 Å shorter than the Au−Au distance in metallic gold (2.878 Å).

Ethane Elimination from gem-Digold Methyl Complexes. As anticipated, the stability of gem-digold methyl complexes largely depends on the steric shielding provided by the phosphine ligand. Thus, the compound $[Au_2(\mu\text{-}CH_3)(PMe_2Ar^{Xyl2})_2][NTf_2]$ (**4a**) is only stable in dichloromethane solution at −30 °C or below. Above −20 °C, **4a** cleanly converts into $[Au(PMe_2Ar^{Xyl2})_2][NTf_2]$ (**5a**), metallic gold, and ethane (Scheme 5). Complex $[Au_2(\mu\text{-}CH_3)(PMe_2Ar^{Mes2})_2][NTf_2]$ (**4b**) reacts in a similar way, whereas bulkier phosphines provide enhanced stability. As such, compounds $[Au_2(\mu\text{-}CH_3)(PMe_2Ar^{Dipp2})_2][NTf_2]$ (**4c**) and $[Au_2(\mu\text{-}CH_3)(PMe_2Ar^{Tripp2})_2][NTf_2]$ (**4d**), in which the methyl substituents in the lateral aryl rings of the terphenyl moiety have been substituted by *iso*-propyl groups, are fairly stable at room temperature, while complexes **4e** and **4f** remain unaltered for hours even at temperatures up to 80 °C. Thus, the investigated Buchwald phosphines confer enhanced stability to gem-digold methyl species compared to terphenyl-based ligands, most likely as a result of the increased steric shielding provided by the cyclohexyl and *tert*-butyl groups directly bound to the phosphorus center in close proximity to the gold nuclei.

Scheme 5. Thermal Decomposition of Terphenyl and Biaryl Phosphine Methyl-Bridged Digold Complexes (4a−4e) to Gold Bisphosphine (5a−5e)

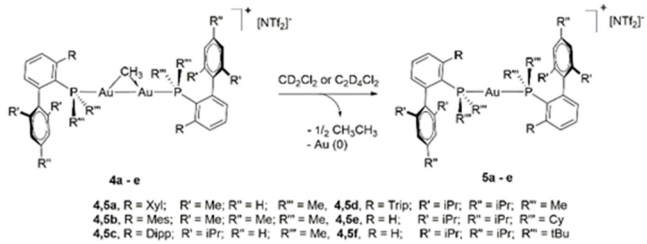

Overall, these observations indicate that kinetic analysis by ^1H and $^{31}P\{^1H\}$ NMR spectroscopy monitoring is facilitated by larger phosphine ligands compared to PPh_3. For instance, heating complex **4e** in dichloroethane at 90 °C enabled us to monitor by NMR spectroscopy its evolution to $[Au(XPhos)_2][NTf_2]$ (**5e**) with concomitant release of ethane and formation of Au(0) (Figure S5). The thermolysis of **4e** follows a second-order dependence on the digold complex with $k_{obs} = 5.2(1) \times 10^{-4}$ M^{-1} s^{-1} at 90 °C (Table 2), as previously observed for the PPh_3-based system. In the case of the more hindered compound **4f**, this reaction does not take place at 100 °C, and intractable digold decomposition occurs at temperatures above 100 °C where the formation of methane, instead of ethane, was observed (Figure S14). This finding indicates that C−C coupling is likely not viable in the most sterically constrained digold system studied herein. This seems to be consistent with a second-order dependence on digold complex concentration during ethane formation, which might imply the need for more than two gold nuclei in close proximity along the reaction coordinate (see below for additional discussion). Similar to complex **4e**, ethane elimination from terphenyl-ligated gem-digold methyl complexes follows a second order dependence on **4a−4d** (Figure 7a; see the Supporting Information). Kinetic studies provide rates for ethane elimination from the more sterically hindered **4c** and **4d** of $k_{obs} = 4.8(3) \times 10^{-3}$ and $2.0(1) \times 10^{-2}$ M^{-1} s^{-1} at 50 °C, respectively. In contrast, the rates of ethane elimination from **4a** and **4b** had to be analyzed at lower temperatures (0 °C), resulting in rates of $k_{obs} = 9.8(3) \times 10^{-2}$ and $4.9(1) \times 10^{-1}$ M^{-1} s^{-1} at 0 °C, respectively. The corresponding half-life ($t_{1/2}$) values associated with these kinetic parameters at the working temperatures are approximately 260 (**4a**, 0 °C), 800 (**4b**, 0 °C), 5600 (**4c**, 50 °C), and 13 000 (**4d**, 50 °C) s.

Table 2 collects the corresponding activation barriers for C−C coupling from the methyl-bridged complexes **4a−4e**, which

Table 1. Summary of Selected Bond Distances of the gem-Digold Methyl Complexes

gem-digold methyl complexes	Au−arene[a] (Å)	Au−Au (Å)	Au−*ipso* carbon of arene (Å)	Au−CH_3 (Å)
$[Au_2(\mu\text{-}CH_3)(PMe_2Ar^{Dipp2})_2][BAr_F]$[34] (**4c**)	3.259(3)	2.7120(8)	3.027(3)	2.210(5)
	3.321(3)	2.7120(8)	3.102(3)	2.227(4)
$[Au_2(\mu\text{-}CH_3)(XPhos)_2][NTf_2]$[b] (**4e**)	3.400(2)	2.7330(4)	3.093(5)	2.215(5)
	3.465(2)	2.7330(4)	3.185(5)	2.238(5)
$[(Au)_2(\mu\text{-}CH_3)(^tBuXPhos)_2][NTf_2]$ (**4f**)	3.366(3)	2.7765 (5)	3.082(8)	2.207(8)
	3.413(3)	2.7765 (5)	3.406(8)	2.204(9)

[a]Distance from Au to the centroid of the arene rings. [b]Average over three independent molecules present in the asymmetric unit.

https://dx.doi.org/10.1021/jacs.0c11296
J. Am. Chem. Soc. 2021, 143, 2509−2522

Table 2. Summary of Kinetic Data for Ethane Elimination from gem-Digold Complexes 4a−4e

compound	T (°C)	k (M^{-1} s^{-1})	$\Delta G^{‡}$ (kcal/mol)
$[Au_2(\mu\text{-}CH_3)(PMe_2Ar^{Xyl2})_2][NTf_2]$ (**4a**)	0	$9.8(3) \times 10^{-2}$	17.2(1)
$[Au_2(\mu\text{-}CH_3)(PMe_2Ar^{Mes2})_2][NTf_2]$ (**4b**)	0	$4.9(1) \times 10^{-2}$	17.6(1)
$[Au_2(\mu\text{-}CH_3)(PMe_2Ar^{Dipp2})_2][NTf_2]$ (**4c**)	50	$4.8(3) \times 10^{-3}$	22.4(5)
$[Au_2(\mu\text{-}CH_3)(PMe_2Ar^{Tipp2})_2][NTf_2]$ (**4d**)	50	$2.0(1) \times 10^{-3}$	22.9(4)
$[Au_2(\mu\text{-}CH_3)(XPhos)_2][NTf_2]$ (**4e**)	90	$5.2(1) \times 10^{-4}$	26.4(3)
$[Au_2(\mu\text{-}CH_3)(^tBuXPhos)_2][NTf_2]$ (**4f**)	100[a]	N.A.	N.A.

[a]Methane formation observed instead; N.A. (not available).

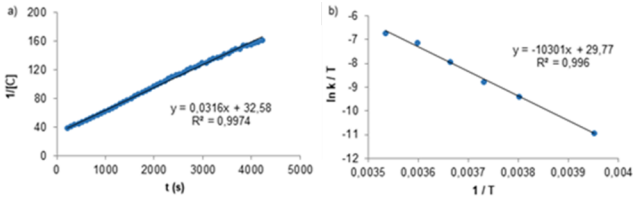

Figure 7. (a) Second-order kinetic representation for the consumption of **4a** at −5 °C in CD_2Cl_2. (b) Eyring plot for ethane formation from gem-digold methyl $[Au_2(\mu\text{-}CH_3)(PMe_2Ar^{Xyl2})_2][NTf_2]$ (**4a**).

range from 17.2 kcal/mol at 0 °C for **4a** to 26.4 kcal/mol at 90 °C for **4e**. To complete these studies, we monitored the evolution of ethane from the gem-digold complex **4a** in the temperature interval from −20 to 10 °C. An Eyring analysis provided activation parameters of $\Delta H^{‡}$ = 20.5 ± 1.3 kcal/mol and $\Delta S^{‡}$ = 11.9 ± 4.8 e.u. (Figure 7b), which correspond to $\Delta G_{298}{}^{‡}$ = 16.9 ± 2.7 kcal/mol.

To obtain a deeper insight into the nature of the Au species involved in C−C coupling processes, we first considered whether dissociation of complexes **4** into their monometallic components,[59] namely, neutral methyl compounds **1** and triflimide species of type $Au(PR_2Ar')(NTf_2)$, might be relevant. To check the viability of such equilibria, we explored exchange processes of the methyl bridge in compound **4a**. In a first experiment, we examined the exchange between **1a** and **4a** at variable temperatures. For experimental convenience, we accessed an equimolar mixture of both species by adding 0.33 equiv of $[Ph_3C][B(C_6F_5)_4]$ to **1a** at −40 °C. Under these conditions, one-third of the neutral methyl compound is

Scheme 6. (a) Dynamic Me/Me Exchange Equilibrium between $[Au_2(\mu\text{-}CH_3)(PMe_2Ar^{Xyl2})_2][NTf_2]$ (4a) and $Au(CH_3)(PMe_2Ar^{Xyl2})$ (1a) Species at −40°C; (b) C−C Coupling and Product Distribution in the Reaction between $Au(C_2H_5)(PMe_2Ar^{Xyl2})$ (2a) and $[Au_2(\mu\text{-}CH_3)(PMe_2Ar^{Xyl2})_2][NTf_2]$ (4a); and (c) C−C Coupling and Product Distribution in the Reaction between $Au(C_6H_5)(PMe_2Ar^{Xyl2})$ (3a) and $[Au_2(\mu\text{-}CH_3)(PMe_2Ar^{Xyl2})_2][NTf_2]$ (4a)

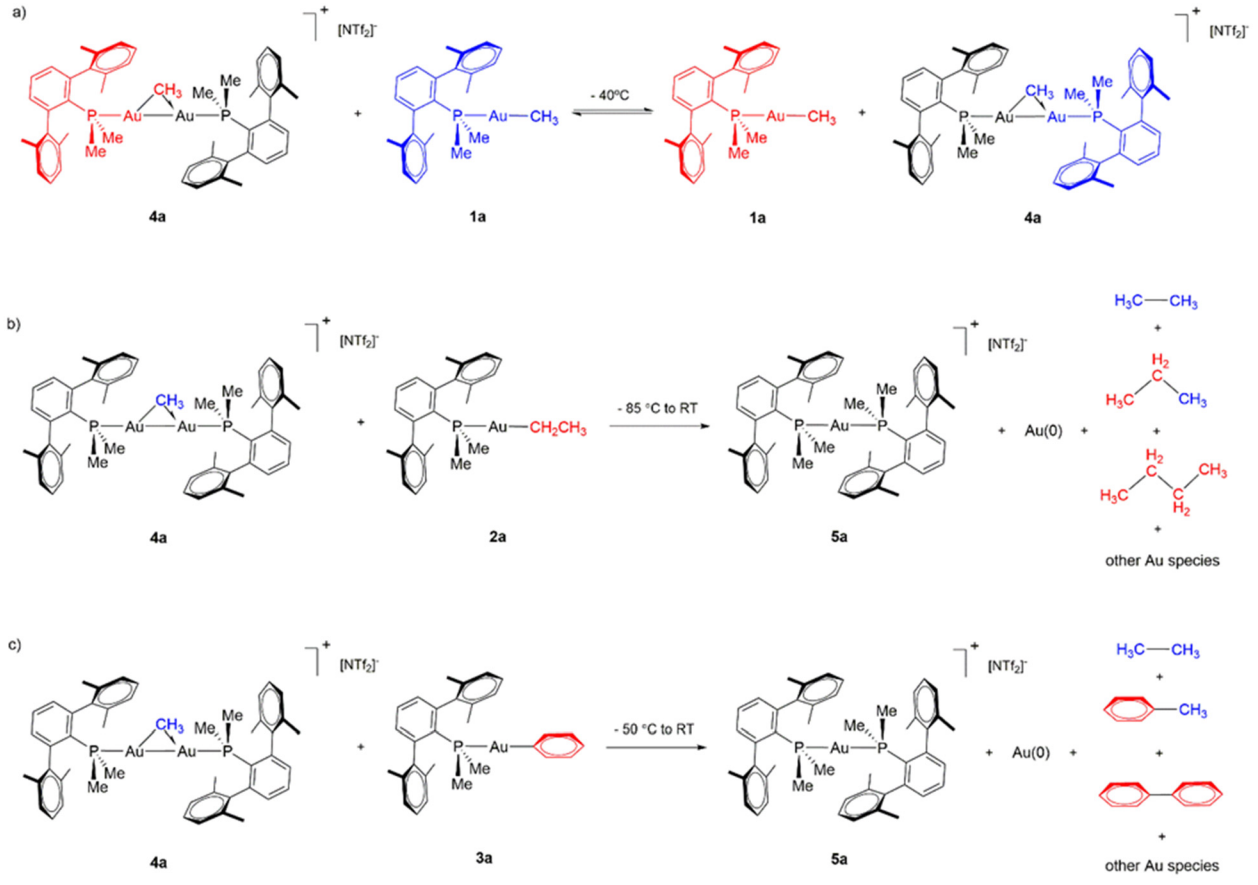

https://dx.doi.org/10.1021/jacs.0c11296
J. Am. Chem. Soc. 2021, 143, 2509−2522

transformed by methyl abstraction into a cationic gold species that is immediately trapped by unreacted **1a** to provide gem-digold **4a**. Variable temperature ^{1}H and $^{31}P\{^{1}H\}$ NMR spectroscopy analysis revealed dynamic behavior in solution (Figure S10), which we attribute to the exchange equilibrium depicted in Scheme 6a. It was possible to identify **4a** by a $^{31}P\{^{1}H\}$ NMR resonance at 0.1 ppm recorded at −85 °C, whereas a broad signal at 21.1 ppm was assigned to **1a**. These signals coalesce at approximately −40 °C, while the major component when reaching 25 °C is the homoleptic bisphosphine compound **5a** that accompanies ethane formation. We further investigated this dynamic behavior by DFT methods (see the Supporting Information for details). Calculations indicate that dissociation of the dinuclear species $[Au_2(\mu\text{-}CH_3)(PMe_2Ar^{Xyl2})_2][NTf_2]$ (**4a**) into the corresponding fragments, $Au(CH_3)(PMe_2Ar^{Xyl2})$ (**1a**) and $Au(PMe_2Ar^{Xyl2})(NTf_2)$, is only slightly endergonic (ΔG = +0.5 kcal/mol), in agreement with our experimental results. The kinetic profile of ethane evolution in these equimolar mixtures is identical, within the experimental error, to that of pure **4a**.

This suggests that, even if carbon−carbon coupling takes place from a trimetallic species involving the participation of compounds **1**, the required dissociation of gem-digold methyl compounds **4** into compounds **1** and $[Au(PR_2Ar')]^+$ is not likely kinetically relevant.

Substituting methyl compound **1a** by its related ethyl (**2a**) and phenyl (**3a**) derivatives showed the formation of cross-coupling products (Scheme 6b,c). In the case of **2a**, the formation of propane and butane was apparent by ^{1}H NMR spectroscopy, while in the reaction between **4a** and **3a** the formation of ethane, biphenyl, and toluene was detected in comparable amounts. GC-MS analysis of solution and gas headspace provided further evidence for cross coupling, since variable amounts of ethane, propane, and butane were measured from the reaction between **2a** and **4a** (Figure S21). In both cases, the main homogeneous gold-containing species when reaching room temperature is **5a**.

To gather more information on the exchange between bridging and terminal hydrocarbyl substituents present in gem-digold and neutral compounds, we examined the reaction depicted in Scheme 6b at variable temperatures (Figure 8). A solid mixture of **2a** and **4a** in equimolar amounts was dissolved in CD_2Cl_2 at −40 °C to allow the exchange to take place and then cooled to −85 °C. At the latter temperature, the exchange process is halted, and a variety of gold-containing products are identified by $^{31}P\{^{1}H\}$ NMR. These include the neutral hydrocarbyl compounds **1a** and **2a** and their corresponding gem-digold species **4a** and $[Au_2(\mu\text{-}CH_2CH_3)(PMe_2Ar^{Xyl2})_2]$ (**6a**), whose broad resonances were recorded at 21.2, 21.9, 0.1, and 1.4 ppm, respectively. Also, sharp signals due to $Au(PMe_2Ar^{Xyl2})(NTf_2)$ and $[Au(PMe_2Ar^{Xyl2})_2][NTf_2]$ (**5a**) were identified at −4.2 and 10.8 ppm, respectively. The latter likely results from local solution warm-up during sample handling. Increasing the temperature to −40 °C results in coalescence of all prior resonances except for that of **5a**, which is clearly not involved in the exchange process. Further raising the temperature to 25 °C leads to full consumption of gold precursors and quantitative formation of bisphosphine compound **5a** along with the appearance of solid Au(0). Similarly, rapid exchange between **4a** and **3a** is evinced by immediate conversion of an equimolar mixture of those compounds into **1a** and $[Au_2(\mu\text{-}C_6H_5)(PMe_2Ar^{Xyl2})_2]$ (**7a**) (Figure S11).

Having in mind that the above dynamic behavior reveals the presence of compounds **1**, **4**, and $Au(PR_2Ar')(NTf_2)$ in solution, and also considering the fact that ethane evolution follows a second-order dependence on bridging methyl complexes **4**, we considered three possible routes (Scheme 7). In the first, reductive coupling from two neutral gold

Scheme 7. Potential Routes for Ethane Evolution with Regards to the Gold Coupling Partners

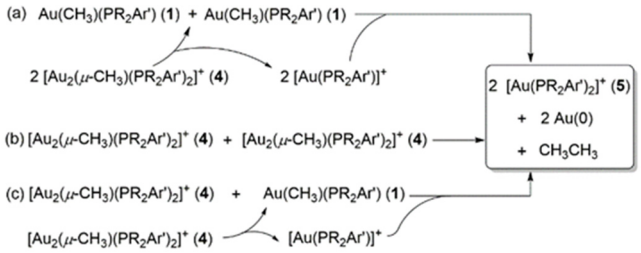

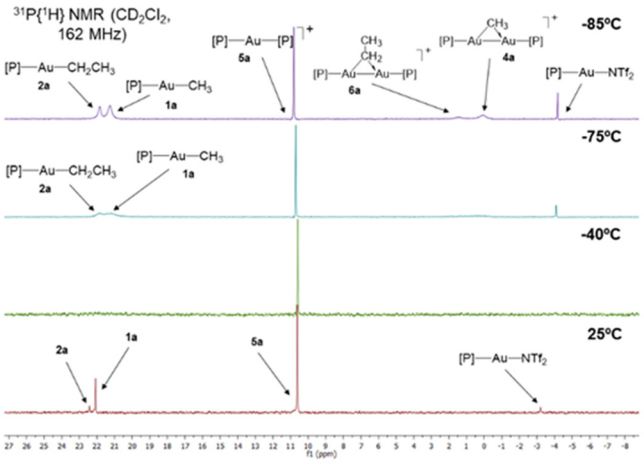

Figure 8. Variable temperature of exchange processes between $Au(C_2H_5)(PMe_2Ar^{Xyl2})$ (**2a**) and $[Au_2(\mu\text{-}CH_3)(PMe_2Ar^{Xyl2})_2][NTf_2]$ (**4a**) monitored by $^{31}P\{^{1}H\}$ NMR spectroscopy.

methyl compounds of type **1** may take place, similar to prior work by Kochi and co-workers (Scheme 7a).[31,32] However, it is important to highlight two distinctive features of our studies that contrast with those prior reports. First, reductive coupling from $Au(CH_3)(PPh_3)$ only occurred at high temperatures (~100 °C), while C−C bond formation from bridging digold complexes **4** is more facile. In fact, the C−C coupling reaction readily proceeds at temperatures as low as −60 °C in the case of the PPh_3-based system (Figures S8 and S9). Second, whereas a first-order dependence on gold was demonstrated for reductive coupling from $Au(CH_3)(PPh_3)$,[31,32] with phosphine dissociation toward "AuMe" as the rate-determining step, we have determined a second-order dependence on digold compounds **4** during ethane evolution. These observations suggest different operating mechanisms in the two cases, a notion that is further supported by DFT methods based on the PMe_2Ar^{Xyl2} system. In agreement with Kochi's findings, the computed reaction free energy for phosphine dissociation at **1a** is +32.1 kcal/mol, much higher than the experimentally determined activation free energy for the overall process ($\Delta G_{298}^{\ddagger}$ = 16.9 ± 2.7 kcal/mol, see above). Phosphine dissociation from **4a** to yield $[Au_2(\mu\text{-}CH_3)$-

https://dx.doi.org/10.1021/jacs.0c11296
J. Am. Chem. Soc. 2021, 143, 2509−2522

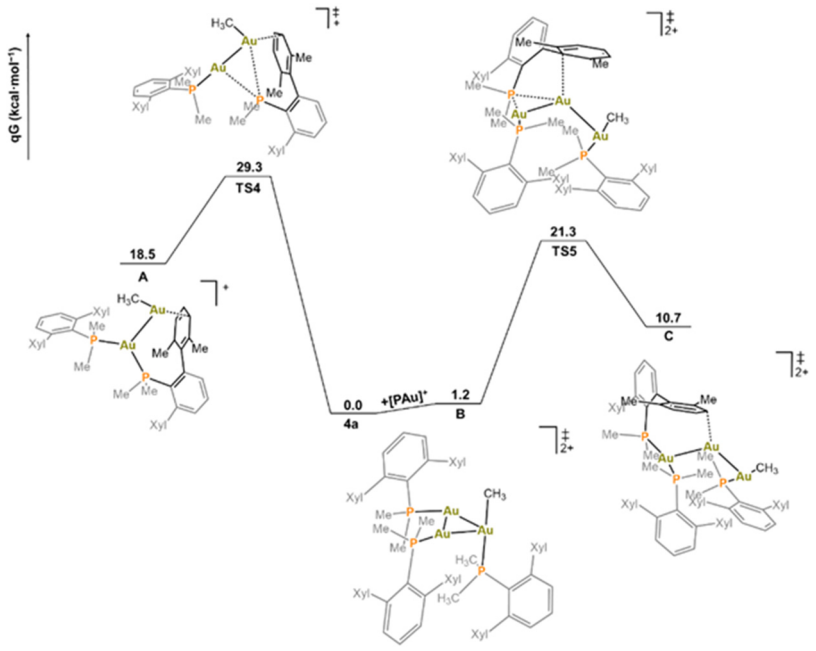

Figure 9. Free energy profile for $[Au(PMe_2Ar^{Xyl2})]^+$-promoted phosphine migration and formation of masked "AuMe" from $Au(CH_3)(PMe_2Ar^{Xyl2})$ (**1a**, left) or $[Au_2(\mu\text{-}CH_3)(PMe_2Ar^{Xyl2})_2]^+$ (**4a**, right) complexes; calculated at the ωB97X-D/6-31G(d,p) level.

$(PMe_2Ar^{Xyl2})][NTf_2]$, where the metal−metal and metal−arene interactions could stabilize the unsaturated gold center, presented a similarly high value [+31.1 kcal/mol; Figure S20 (including a molecule of CH_2Cl_2 in the calculation to compensate the unsaturation of the metal center results in higher reaction free energies: +33.3 and +42.6 kcal/mol for phosphine dissociation from **1a** and **4a**, respectively)]. As anticipated, these data confirm a dissimilar C−C coupling mechanism for compounds **4** compared to that exhibited by monometallic gold-alkyl species.

An alternative route consists of two gem-digold methyl fragments **4** approaching to facilitate the C−C coupling event (Scheme 7b). However, a third pathway to consider, in view of the Coulombic repulsion derived from the approach of two cationic species in route b, is the reaction between **4** and its corresponding neutral methyl species **1** formed by dissociation of a second molecule of **4** into their monometallic fragments (Scheme 7c). First, we explored computationally the direct coupling of methyl groups between two molecules of **4a** (route a) as well as between **4a** and **1a** (route b) by relaxed potential energy scans. These studies indicate that those pathways are unfeasible, both in the singlet and triplet state. We also evaluated the possibility of accessing the hypothetical Au(III) species $[Au(CH_3)_2(PMe_2Ar^{Xyl2})][NTf_2]$ from the above routes, since reductive coupling of ethane with such a complex should be accessible.[18,29,30] In fact, we found a feasible barrier (+16.1 kcal/mol) for ethane formation from the hypothetical Au(III) complex $[Au(CH_3)_2(PMe_2Ar^{Xyl2})][NTf_2]$ (Figure S15). However, $[Au(CH_3)_2(PMe_2Ar^{Xyl2})][NTf_2]$ would be formed alongside the digold(0) species $[Au_2(PMe_2Ar^{Xyl2})_2]$, with these species being 42.1 kcal/mol higher in energy than its precursors, rendering this pathway inaccessible under the reaction conditions (Figure S15). Similarly, CH_3^+ transfer[36] from **4a** to **1a** presents a computed transition state at +47.0 kcal/mol (**TS1** in Figure S16). In addition, we examined reductive coupling from the hypothetical trinuclear species derived from the above CH_3^+ transfer; a transition state at +33.6 kcal/mol was found (**TS2** in Figure S16), further suggesting that this pathway is unaffordable.

Finally, we considered the possible involvement of gold carbene ($AuCH_2$) and hydride (AuH) species,[60] potentially formed by hydride abstraction from Au-methyl complexes. However, the free energy cost to access these high-energy intermediates is calculated to be at least +36.2 kcal/mol (Figures S17 and S18), incompatible with the determined activation parameters. To further rule out this mechanistic route, we carried out an additional experiment with isotopically labeled $[Au(CD_3)(PMe_2Ar^{Xyl2})]$ (**1a-*d*$_3$**; see the Supporting Information for details). Treating an equimolar mixture of **1a** and **1a-*d*$_3$** with 2 equiv of $Au(PMe_2Ar^{Xyl2})(NTf_2)$ yielded an approximate statistic mixture of CH_3CH_3, CH_3CD_3, and CD_3CD_3 (Figure S12), without further observable H/D scrambling, thus excluding the involvement of gold methylidene species.

Having ruled out the most direct mechanisms involving **1a** and **4a**, we decided to interrogate the participation of compounds $Au(PR_2Ar')(NTf_2)$, especially in consideration of the experimental results indicating that such complexes are accessible under the reaction conditions (see above). These compounds serve as a source of electrophilic $[Au(PR_2Ar')]^+$ fragments[61,62] and, as such, might facilitate or drive phosphine dissociation from other Au complexes. Potential phosphine dissociation is implicated from straightforward ligand exchange experiments (see Figure S13), and since it was proposed as the rate-limiting step in Kochi's earlier system,[31,32] it is conceivable that it could also play a role for C−C coupling from compounds **4**. To examine this, we monitored ethane evolution from **4a** in the presence of 3 equiv of $Au(PMe_2Ar^{Xyl2})(NTf_2)$, though this excess of gold-triflimide did not have notable effects on the rate of ethane formation. This was, however, not surprising in line with our computational results, where the larger barrier originates after binding of $[Au(PMe_2Ar^{Xyl2})]^+$ to **4a**. Nonetheless, even if $Au(PMe_2Ar^{Xyl2})(NTf_2)$ is required to facilitate phosphine

https://dx.doi.org/10.1021/jacs.0c11296
J. Am. Chem. Soc. 2021, 143, 2509−2522

dissociation, its presence may also affect the observed rate of ethane evolution in an opposite manner by reducing the concentration of $Au(CH_3)(PMe_2Ar^{Xyl2})$ (**1a**) in solution, the latter species also being required for C−C coupling. This is because $[Au_2(\mu\text{-}CH_3)(PMe_2Ar^{Xyl2})_2][NTf_2]$ (**4a**) is in dynamic equilibrium in solution with **1a** and $Au(PMe_2Ar^{Xyl2})(NTf_2)$, as discussed above. To circumvent the influence of added $Au(PMe_2Ar^{Xyl2})(NTf_2)$ on that equilibrium, we investigated the effect of adding 5 equiv of BPh_3 as an alternative and less disruptive Lewis acid that could facilitate phosphine dissociation. While ethane evolution proceeded at a rate ($t_{1/2}$ = 340 s) comparable to that of pure **4a** ($t_{1/2}$ = 260 s), we did observe a distinctive change in the kinetic profile. More precisely, this experiment revealed a first-order kinetic dependence on **4a** (Figure S7), in contrast to the second-order profile observed when the consumption of the latter was monitored in pure form.

Next, we directed our efforts to examining, by computational means, the role of $Au(PMe_2Ar^{Xyl2})(NTf_2)$ on the pathways and energetics for the formation of ethane (Figure 9). Since we attribute a Lewis acidic role to this fragment, as supported by our experiments with BPh_3, we first studied BH_3 as a simplified Lewis acid. Thus, we examined the reaction between BH_3 and complex $Au(CH_3)(PMe_2Ar^{Xyl2})$ (**1a**). The formation of a Au−BH_3 adduct is slightly exergonic (ΔG = −0.9 kcal/mol), from which the transition state for the formation of a P−B bond (**TS3**) lies at +16.2 kcal/mol above the independently computed **1a** and BH_3, giving the product at −7.4 kcal/mol (Figure S19). Encouraged by this result, we studied the analogous process with cation $[Au(PMe_2Ar^{Xyl2})]^+$ instead of BH_3 as the Lewis acid.[63] A transition state for that process (**TS4**) was found at +29.3 kcal/mol, leading to the formation of a species of formula $[(PMe_2Ar^{Xyl2})_2AuAu(CH_3)]^+$, **A** in Figure 9, that lies at +18.5 kcal/mol and represents a form of masked "AuMe" stabilized by aurophilic and metal−arene interactions with the $[Au(PMe_2Ar^{Xyl2})_2]^+$ fragment. Nonetheless, the large barrier renders this process inaccessible from **4a**, in agreement with the experimentally determined second-order dependence on its concentration.

To account for the second-order dependence on **4a**, we considered its initial dissociation into **1a** and $Au(PMe_2Ar^{Xyl2})(NTf_2)$, the latter providing 1 equiv of cation $[Au(PMe_2Ar^{Xyl2})]^+$ amenable to bind a second molecule of **4a**. The resulting trigonal dicationic adduct $[Au_3(\mu\text{-}CH_3)(PMe_2Ar^{Xyl2})_3]^{2+}$ (**B**) plus **1a** are only 1.2 kcal/mol above two molecules of **4a** (Figure 9). From trimetallic adduct **B**, the transition state for the formal transfer of a phosphine ligand between gold atoms was found at +21.3 kcal/mol (**TS5**), close enough to the experimentally determined value for the overall process of ethane evolution. This transition state gives trinuclear species **C** at +10.7 kcal/mol, from which dissociation of **5a** is thermodynamically accessible (ΔG = +2.5 kcal/mol). This would render the bimetallic intermediate $[Au_2(CH_3)(PMe_2Ar^{Xyl2})]^+$ (Figure S20), which is reminiscent of the proposed highly reactive "AuMe" fragment proposed by Kochi.[31,32] From such a reactive fragment, masked as $[Au_2(CH_3)(PMe_2Ar^{Xyl2})]^+$, it is expected that the approach of **1a** would result in ethane elimination and formation of colloidal gold, not necessarily in that order.

Our combined experimental/computational approach led us to propose the mechanistic picture for C−C coupling at gem-digold compounds **4** depicted in Scheme 8. Compounds **4** readily dissociate in solution to form **1** and $Au(PR_2Ar')(NTf_2)$, the latter functioning as a Lewis acid to favor phosphine migration from a second molecule of **4** by forming a trimetallic intermediate of type **B**.[64] Following the release of diphosphine compounds **5**, the resulting masked "AuMe" fragment reacts with **1a** to liberate ethane with concomitant formation of elemental Au, eventually leading to the formation of Au nanoparticles. In this picture, phosphine migration from **4a** constitutes the rate-limiting step of the overall process, in analogy to the previously proposed mechanism for reductive coupling from $Au(CH_3)(PPh_3)$.[31,32] In contrast, the remarkable acceleration observed for C−C coupling in compounds **4** compared to **1** seems to be the result of stabilization of key intermediates by the presence of aurophilic interactions combined with the Lewis acidic character of $[Au(PR_2Ar')]^+$ that enables phosphine migration, thus representing an example of rate acceleration by polymetallic entities compared to monometallic counterparts.[65−67]

Scheme 8. Proposed Mechanism for the Reductive Coupling of Ethane from gem-Digold Compounds 4

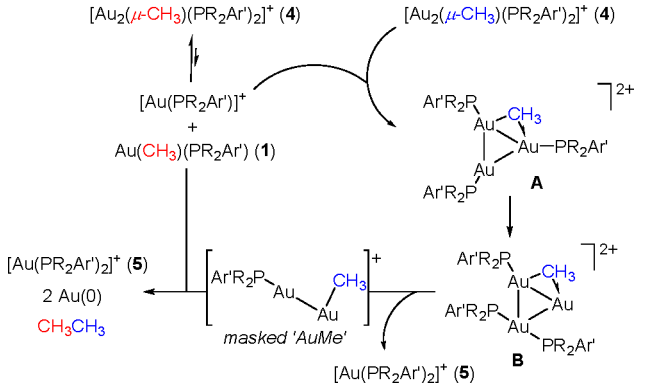

CONCLUSIONS

Au-mediated C−C coupling processes have rapidly emerged as versatile and powerful strategies for organic synthesis. Despite numerous reports on the synthetic applicability of gold catalysts, mechanistic understanding has evolved at a slower pace. Previous studies have placed the Au(I)/Au(III) redox couple at the heart of all these transformations, while mechanistic investigations on C−C coupling processes without the apparent advent of Au(III) species is lacking. Herein, we have demonstrated that gem-digold methyl complexes $[Au_2(\mu\text{-}CH_3)(PR_2Ar')_2][NTf_2]$ (**4**) promote the homocoupling of the bridging methyl fragments to produce ethane at a remarkably higher rate than from its parent neutral species $Au(CH_3)(PR_2Ar')$ (**1**). We have also demonstrated that this approach permits the heterocoupling of the bridging methyl group with ethyl and phenyl fragments. The stability of compounds **4** toward reductive homocoupling is highly dependent on the steric bulk of the phosphine ligand. Whereas the system based on PPh_3 readily liberates ethane at −40 °C, those bearing terphenyl phosphines (PMe_2Ar') exhibit considerably enhanced stability, which is further increased by the use of the more hindered XPhos and ^{t}BuXPhos, the latter being unable to mediate C−C coupling even at 90 °C. Our kinetic studies revealed second-order dependence on gem-digold methyl complexes **4** during ethane evolution, whereas a distinctive change toward a first-order dependence on the latter was ascertained in the presence of excess BPh_3 as an external Lewis acid. On the basis of our experimental studies combined with

https://dx.doi.org/10.1021/jacs.0c11296
J. Am. Chem. Soc. 2021, 143, 2509−2522

DFT computational methods we have proposed a mechanism that involves rapid dissociation of a molecule of $[Au_2(\mu\text{-}CH_3)(PMe_2Ar')_2][NTf_2]$ (**4**) toward $Au(PMe_2Ar')(NTf_2)$ and $Au(CH_3)(PMe_2Ar')$ (**1**). While $Au(PMe_2Ar')(NTf_2)$ mediates phosphine migration from a second molecule of **4** via a trimetallic intermediate, compound **1** is proposed to react with the resulting highly reactive and masked "AuMe" fragment to effect the C−C coupling event, most likely by a multinuclear gold species. These studies highlight the relevance of multimetallic mechanisms in mediating uncommon transformations, herein also boosting the rate at which the C−C coupling transformation occurs.

EXPERIMENTAL SECTION

General Methods. Unless otherwise noted, all reactions and manipulations were performed under a nitrogen atmosphere in a glovebox or using standard Schlenk techniques with dried and degassed solvents. All solvents were purified via a solvent purification system or by common distillation techniques: Dichloromethane (CH_2Cl_2) was distilled under nitrogen over CaH_2. Toluene (C_7H_8), benzene (C_6H_6), *n*-hexane (C_6H_{14}), and *n*-pentane (C_5H_{12}) were distilled under nitrogen over sodium. Tetrahydrofuran (THF) and diethyl ether were distilled under nitrogen over sodium/benzophenone. Benzene (C_6D_6) was dried over sodium, while $CDCl_3$ and CD_2Cl_2 were dried over molecular sieves (4 Å) and distilled under nitrogen. Compounds PMe_2Ar',[68] AuCl(THT) (THT = tetrahydrothiophene),[69] $Au(PPh_3)(NTf_2)$,[70,71] $Au(PPh_3)(NO_3)$,[72,73] AuCl(XPhos),[74] AuCl(ᵗBuXPhos),[75] $Au(XPhos)(NTf_2)$,[76−78] Au(ᵗBuXPhos)(NTf_2),[78] $AuCl(PMe_2Ar^{Xyl2})$,[62] $AuCl(PMe_2Ar^{Dipp2})$,[46] $AuCl(PMe_2Ar^{Tripp2})$,[79] $Au(PMe_2Ar^{Xyl2})(NTf_2)$,[62] $Au(PMe_2Ar^{Dipp2})(NTf_2)$,[46] $Au(PMe_2Ar^{Tripp2})(NTf_2)$,[79] $Au(CH_3)(PMe_2Ar^{Dipp2})$[46] (**1c**), and $[Au_2(\mu\text{-}CH_3)(PMe_2Ar^{Dipp2})_2][NTf_2]$[46] (**4c**) were prepared according to previously reported procedures. Compounds **1e** and **1f** were prepared according to the general method described below in yields of around 75%, exhibiting identical spectroscopic data to those previously reported. $Au(CH_3)(XPhos)$[78] and $Au(CH_3)$(ᵗBuXPhos)[80] were prepared by an alternative method of the published procedures and fully characterized. Methyl(triphenylphosphine)gold(I), chloro(dimethylsulfide)gold(I), silver bis(trifluoromethanesulfonyl)imide acetonitrile adduct, chlorotriphenylphosphinegold(I), 2-dicyclohexylphosphino-2′,4′,6′-triisopropylbiphenyl (XPhos), and 2-di-*tert*-butylphosphino-2′,4′,6′-triisopropylbiphenyl (ᵗBuXPhos) were purchased from STREM Chemicals and were used as received. Other chemicals were purchased from Sigma-Aldrich and used as received. All new compounds have been characterized by ^{1}H NMR spectroscopy, ^{31}P NMR spectroscopy, ^{13}C NMR spectroscopy, and elemental analysis (see Figure 10). Solution NMR spectra were recorded on Varian Inova 600 or 500 MHz or on Bruker AMX-300, DRX-400, DRX-500, and Avance III 800 MHz spectrometers. Spectra were referenced to external $SiMe_4$ or using the residual proton solvent peaks as internal standards (^{1}H NMR experiments), or the characteristic resonances of the solvent nuclei (^{13}C NMR experiments), while ^{31}P was referenced to H_3PO_4. Spectral assignments were made by routine one- and two-dimensional NMR experiments where appropriate. For elemental analyses, the LECO TruSpec CHN elementary analyzer and PerkinElmer 2400 Series II analyzer were utilized. GC analysis was performed using a Shimadzu GCMSQP2010-Plus instrument equipped with a PoraBOND-Q capillary column (25 m, 0.25 mm i.d., 3.0 μm film thickness, Agilent Technologies). Helium carrier gas was supplied at a head pressure of 10 psi to provide an initial flow rate of 1.4 mL/min. A 1 mL injection with a split ratio of 1:10 was employed. GC temperature was initially held at 40 °C for 1 min and gradually increased to 120 °C at 5 °C/min. Full-scan mass spectra were collected from 5 to 70 m/z at a data acquisition rate of 3.5 spectra/s. The MS transfer line was held at 250 °C, and the ion source temperature was 200 °C. Samples analyzed by transmission electron microscopy (TEM) were prepared by dispersing the powders in cyclohexane or hexanes (99.5%, anhydrous, Sigma-Aldrich) and sonicating for 1 min before mounting on Cu-supported holey carbon grids. The Au samples were imaged using an FEI Titan 80-300 operating at 300 kV. The structures of compounds **1a**, **1e**, **1f**, **2a**, **3a**, **4e**, **4f**, and Au(ᵗBuPhos)(NTf_2) have been authenticated by X-ray diffraction studies and their corresponding CIF files deposited in the Cambridge Crystallographic Data Centre with nos. 2024182−2024189.

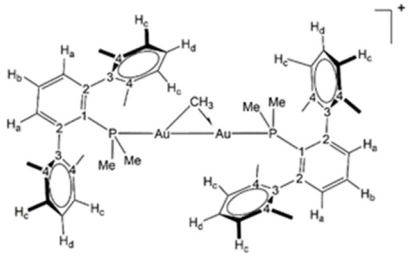

Figure 10. Labeling scheme used for ^{1}H and ^{13}C{^{1}H} NMR assignments.

General Synthesis of Compounds 1. A suspension of the corresponding gold chloride precursor $AuCl(PR_2Ar')$ (0.20 mmol) in toluene (10 mL) was cooled to −78 °C, and a solution of MeMgX (X = Cl or Br; 2.5 equiv) in toluene was added dropwise. The mixture was allowed to warm up slowly for 16 h. The volatiles were removed in vacuo, and the residue was extracted with benzene for **1a−1d** or pentane for **1e−1f**. Evaporation of the organic solvent led to compounds **1a−1f** as white powders in around 60−80% yields. Isotopologue **1a-d_3** was synthesized by the same procedure using freshly prepared CD_3MgI.[81] Suitable crystals of compounds **1** can be obtained by slow solvent evaporation from pentane/Et_2O or pentane/dichloromethane solutions. Spectroscopic and analytical data for selected compounds (others can be found in the SI). Compound **1a**. Yield: 84 mg, 75%. Anal. Calcd for $C_{25}H_{30}AuP$: C, 53.8; H, 5.4. Found: C, 53.4; H, 5.5. ^{1}H NMR (400 MHz, CD_2Cl_2, 25 °C) δ: 7.53 (td, 1 H, $^5J_{HP}$ = 1.7 Hz, H_b), 7.23 (t, 2 H, H_d), 7.14 (d, 4 H, H_c), 7.07 (dd, 2 H, $^4J_{HP}$ = 2.9 Hz, H_a), 2.13 (s, 12 H, CH_3(Xyl)), 1.02 (d, 6 H, $^2J_{HP}$ = 7.7 Hz, PMe_2), −0.08 (d, 3 H, $^3J_{HP}$ = 8.2 Hz, $AuCH_3$). All aromatic couplings are of ca. 7.5 Hz. ^{13}C{^{1}H} NMR (100 MHz, CD_2Cl_2, 25 °C) δ: 147.0 (d, $^2J_{CP}$ = 10 Hz, C_2), 142.3 (d, $^4J_{CP}$ = 4 Hz, C_3), 137.2 (C_4), 131.8 (d, $^1J_{CP}$ = 35 Hz, C_1), 131.6 (d, $^4J_{CP}$ = 3 Hz, CH_b), 131.5 (d, $^3J_{CP}$ = 7 Hz, CH_a), 128.6 (CH_d), 128.4 (CH_c), 22.4 (CH_3(Xyl)), 16.8 (d, $^1J_{CP}$ = 30 Hz, PMe_2), 4.7 (d, $^2J_{CP}$ = 100 Hz, $AuCH_3$). ^{31}P{^{1}H} NMR (162 MHz, CD_2Cl_2, 25 °C) δ: 22.1. MS (ESI) m/z: calcd for $M(Na)^+$, 581.2; expt., 581.4. Compound **1d**. Yield: 106 mg, 70%. Anal. Calcd for $C_{39}H_{58}AuP$: C, 62.1; H, 7.7. Found: C, 62.0; H, 7.5. ^{1}H NMR (300 MHz, CD_2Cl_2, 25 °C) δ: 7.42 (td, 1 H, $^5J_{HP}$ = 1.8 Hz, H_b), 7.15 (dd, 2 H, $^4J_{HP}$ = 3.0 Hz, H_a), 7.08 (s, 4 H, H_c), 2.94 (hept, 2 H, $^3J_{HH}$ = 6.9 Hz, *p*-^{i}Pr(CH)), 2.58 (hept, 4 H, $^3J_{HH}$ = 6.9 Hz, *o*-^{i}Pr(CH)), 1.31 (d, 12 H, $^3J_{HH}$ = 6.9 Hz; d, 12 H, $^3J_{HH}$ = 6.9 Hz, *o*-^{i}Pr(CH_3), *p*-^{i}Pr(CH_3)), 1.07 (d, 6 H, $^2J_{HP}$ = 7.4 Hz, PMe_2), 1.02 (d, 12 H, $^3J_{HH}$ = 6.9 Hz, *o*-^{i}Pr(CH_3)), −0.36 (d, 3 H, $^3J_{HP}$ = 8.2 Hz, $AuCH_3$). All aromatic couplings are of ca. 7.5 Hz. ^{13}C{^{1}H} NMR (125 MHz, CD_2Cl_2, 25 °C) δ: 149.9 (C_5), 146.9 (C_4), 146.6 (d, $^2J_{CP}$ = 11 Hz, C_2), 137.9 (d, $^4J_{CP}$ = 5 Hz, C_3), 133.7 (C_1), 133.4 (d, $^3J_{CP}$ = 7 Hz, CH_a), 129.3 (CH_b), 121.8 (CH_c), 35.1 (*p*-^{i}Pr(CH)), 31.9 (*o*-^{i}Pr(CH)), 26.1 (*o*-^{i}Pr(CH_3)), 24.9 (*p*-^{i}Pr(CH_3)), 23.4 (*o*-^{i}Pr(CH_3)), 17.3 (d, $^1J_{CP}$ = 30 Hz, PMe_2), 5.7 (d, $^2J_{CP}$ = 102 Hz, $AuCH_3$). ^{31}P{^{1}H} NMR (121 MHz, CD_2Cl_2, 25 °C) δ: 19.8. MS (ESI) m/z: calcd for $M(Na)^+$, 777.4; expt., 777.5.

General Synthesis of Compounds 4. A solid mixture of the corresponding methyl gold precursor **1a−1f** (0.0175 mmol) with 1 equiv of its parent compound $[Au(PR_2Ar')][NTf_2]$(0.0175 mmol) was dissolved in CD_2Cl_2 (0.6 mL) under nitrogen at −50 °C to rapidly yield the desired methyl-bridged complex **4a−4f** in a quantitative NMR spectroscopic yield. Characterization of the less stable compounds **4a** and **4b** was carried out by multinuclear NMR spectroscopy at low temperature without further purification. Compounds **4c−4f** were obtained as colorless microcrystalline

https://dx.doi.org/10.1021/jacs.0c11296
J. Am. Chem. Soc. 2021, 143, 2509−2522

substances by precipitation with pentane at −20 °C (**4c**, **4d**) or 25 °C (**4e**, **4f**) in around 90% yields. Alternatively **4a**−**4f** can be prepared in comparable by treating compounds **1a**−**1f** with 1/2 equiv of $[Ph_3C][B(C_6F_5)_4]$ in dichloromethane by an otherwise identical procedure. Spectroscopic and analytical data for selected compounds (others can be found in the SI). Compound **4a**. ^{1}H NMR (400 MHz, CD_2Cl_2, −30 °C) δ: 7.61 (t, 2 H, H_b), 7.25 (t, 4 H, H_d), 7.08 (m, 12 H, H_a, H_c), 1.98 (s, 24 H, CH_3(Xyl)), 1.16 (d, 12 H, $^2J_{HP}$ = 7.7 Hz, PMe_2), 0.45 (br. s, 3 H, $AuCH_3$···Au). All aromatic couplings are of ca. 7.5 Hz. $^{13}C\{^1H\}$ NMR (100 MHz, CD_2Cl_2, −30 °C) δ: 147.1 (d, $^2J_{CP}$ = 11 Hz, C_2), 141.1 (d, $^4J_{CP}$ = 5 Hz, C_3), 136.7 (C_4), 133.3 (CH_b), 131.8 (d, $^3J_{CP}$ = 8 Hz, CH_a), 129.0 (CH_d), 128.2 (CH_c), 127.8 (d, $^1J_{CP}$ = 38 Hz, C_1), 21.9 (CH_3(Xyl)), 16.9 (d, $^1J_{CP}$ = 37 Hz, PMe_2), 0.6 ($AuCH_3$···Au). $^{31}P\{^1H\}$ NMR (162 MHz, CD_2Cl_2, −20 °C) δ: 1.1. Compound **4d**. Anal. Calcd for $C_{101}H_{113}Au_2BF_{20}P_2$: C, 55.8; H, 5.2. Found: C, 56.1; H, 4.9. ^{1}H NMR (400 MHz, CD_2Cl_2, 25 °C) δ: 7.51 (t, 2 H, H_b), 7.17 (dd, 4 H, $^4J_{HP}$ = 3.3 Hz, H_a), 7.05 (s, 8 H, H_c), 2.94 (hept, 4 H, $^3J_{HH}$ = 7.0 Hz, p-^{i}Pr(CH)), 2.41 (hept, 8 H, $^3J_{HH}$ = 6.7 Hz, o-^{i}Pr(CH)), 1.31 (d, 24 H, $^3J_{HH}$ = 7.0 Hz, p-^{i}Pr(CH_3)), 1.22 (m, 36 H,o-^{i}Pr(CH_3), PMe_2), 1.00 (d, 24 H, $^3J_{HH}$ = 6.6 Hz, o-^{i}Pr(CH_3)), 0.25 (s, 3 H, $AuCH_3$···Au). All aromatic couplings are of ca. 7.5 Hz. $^{13}C\{^1H\}$ NMR (100 MHz, CD_2Cl_2, 25 °C) δ: 151.1 (C_5), 147.3 (C_4), 146.8 (d, $^2J_{CP}$ = 12 Hz, C_2), 137.0 (d, $^4J_{CP}$ = 6 Hz, C_3), 134.0 (d, $^3J_{CP}$ = 8 Hz, CH_a), 131.2 (CH_b), 129.4 (d, $^1J_{CP}$ = 56 Hz, C_1), 122.2 (CH_c), 35.0 (p-^{i}Pr(CH)), 32.0 (o-^{i}Pr(CH)), 25.8 (o-^{i}Pr(CH_3)), 24.8 (p-^{i}Pr(CH_3)), 23.5 (o-^{i}Pr(CH_3)), 17.7 (d, $^1J_{CP}$ = 37 Hz, PMe_2), 0.5 (t, $^2J_{CP}$ = 53 Hz, $^1J_{CH}$ = 130 Hz, $AuCH_3$···Au). $^{31}P\{^1H\}$ NMR (162 MHz, CD_2Cl_2, 25 °C) δ: 0.5. MS (ESI) m/z: calcd for M^+, 1493.8; expt., 1493.8. Compound **4e**. Anal. Calcd for $C_{69}H_{101}Au_2F_6NO_4P_2S_2$: C, 50.5; H, 6.2; N, 0.9. Found: C, 50.3; H, 6.2; N, 0.9. ^{1}H NMR (500 MHz, CD_2Cl_2, 25 °C) δ: 7.76 (m, 2 H, H_a), 7.64 (m, 4 H, H_b), 7.22 (m, 2 H, H_c), 7.09 (s, 4 H, H_d), 3.06 (hept, 2 H, $^3J_{HH}$ = 7.1 Hz, o-^{i}Pr(CH), 2.37 (hept, 4 H, $^3J_{HH}$ = 7.0 Hz, p-^{i}Pr(CH)), 2.15 (m, 2 H, Cy(CH_2)), 1.92 (m, 8 H, Cy(CH_2)), 1.85 (m, 2 H, Cy(CH)), 1.46 (m, 8 H, Cy(CH)), 1.44 (d, 12 H, $^3J_{HH}$ = 6.0 Hz, p-^{i}Pr(CH_3)), 1.37 (m, 8 H, Cy(CH)), 1.24 (m, 8 H, Cy(CH)), 1.26 (d, 12 H, $^3J_{HH}$ = 6.0 Hz, o-^{i}Pr(CH_3)), 1.03 (d, 6 H, $^3J_{HH}$ = 6.0 Hz, o-^{i}Pr(CH_3), c), 0.67 (t, 3 H, $^3J_{HP}$ = 2.2 Hz, $AuCH_3$···Au). $^{13}C\{^1H\}$ NMR (201 MHz, CD_2Cl_2, 25 °C) δ: 150.3, 147.1, 146.7 (d, J = 14 Hz), 137.2 (d, J = 6 Hz), 134.2 (d, J = 10 Hz), 133.2, 131.1, 127.8 (d, J = 6 Hz), 127.5 (d, $^2J_{C-P}$ = 48 Hz), 121.3, 37.5 (d, J = 32 Hz), 34.2, 30.8 (d, J = 4 Hz), 30.8, 30.0 (d, J = 4 Hz), 26.8 (d, J = 12 Hz), 26.7 (d, J = 14 Hz), 25.7, 24.9, 24.2, 23.0, 3.1 (t, $^2J_{CP}$ = 48 Hz). $^{31}P\{^1H\}$ NMR (243 MHz, CD_2Cl_2, 25 °C) δ: 39.5.

General Procedure to Measure Kinetic Constants. Kinetic studies were carried using an identical procedure to that described for the general synthesis of compounds **4**, in J-Young NMR tubes under nitrogen atmosphere, and monitoring the disappearance of the *in situ* formed gem-digold methyl compounds **4** by ^{1}H and $^{31}P\{^1H\}$ NMR. Each kinetic experiment was run in triplicates, and average data are given.

■ ASSOCIATED CONTENT

Supporting Information

The Supporting Information is available free of charge at https://pubs.acs.org/doi/10.1021/jacs.0c11296.

Synthesis and characterization of new compounds, X-ray diffraction data, information on kinetic studies, variable temperature analysis and exchange experiments, DFT calculations, and MS and NMR spectra (PDF)

XYZ coordinates (XYZ)

Accession Codes

CCDC 2024182−2024189 contain the supplementary crystallographic data for this paper. These data can be obtained free of charge via www.ccdc.cam.ac.uk/data_request/cif, or by emailing data_request@ccdc.cam.ac.uk, or by contacting The Cambridge Crystallographic Data Centre, 12 Union Road, Cambridge CB2 1EZ, UK; fax: +44 1223 336033.

■ AUTHOR INFORMATION

Corresponding Authors

Jesús Campos − *Instituto de Investigaciones Químicas (IIQ), Departamento de Química Inorgánica and Centro de Innovación en Química Avanzada (ORFEO−CINQA), Universidad de Sevilla and Consejo Superior de Investigaciones Científicas (CSIC), 41092 Sevilla, Spain;* orcid.org/0000-0002-5155-1262; Email: jesus.campos@iiq.csic.es

T. Brent Gunnoe − *Department of Chemistry, University of Virginia, Charlottesville, Virginia 22904, United States;* orcid.org/0000-0001-5714-3887; Email: tbg7h@virginia.edu

Authors

Juan Miranda-Pizarro − *Instituto de Investigaciones Químicas (IIQ), Departamento de Química Inorgánica and Centro de Innovación en Química Avanzada (ORFEO−CINQA), Universidad de Sevilla and Consejo Superior de Investigaciones Científicas (CSIC), 41092 Sevilla, Spain;* orcid.org/0000-0002-0580-7335

Zhongwen Luo − *Department of Chemistry, University of Virginia, Charlottesville, Virginia 22904, United States;* orcid.org/0000-0002-8331-4747

Juan J. Moreno − *Instituto de Investigaciones Químicas (IIQ), Departamento de Química Inorgánica and Centro de Innovación en Química Avanzada (ORFEO−CINQA), Universidad de Sevilla and Consejo Superior de Investigaciones Científicas (CSIC), 41092 Sevilla, Spain;* orcid.org/0000-0003-1809-6170

Diane A. Dickie − *Department of Chemistry, University of Virginia, Charlottesville, Virginia 22904, United States;* orcid.org/0000-0003-0939-3309

Complete contact information is available at: https://pubs.acs.org/10.1021/jacs.0c11296

Author Contributions

[§]J.M.-P. and Z.L. contributed equally.

Notes

The authors declare no competing financial interest.

■ ACKNOWLEDGMENTS

The Gunnoe group acknowledges support from the U.S. National Science Foundation (1800173). The Campos group acknowledges support from the Spanish Ministry of Science and Innovation (Project PID2019-110856GA-I00). The Gunnoe group also acknowledges Jiahan Xie and Robert J. Davis for the TEM analyses. The Campos group acknowledges Carlos Navarro-Gilabert for assistance on ligand synthesis. The two groups acknowledge Prof. Ernesto Carmona for helpful discussions.

■ REFERENCES

(1) Hashmi, A. S. K. Homogeneous Gold Catalysis Beyond Assumptions and Proposals—Characterized Intermediates. *Angew. Chem., Int. Ed.* **2010**, *49*, 5232−5241.

(2) Henrion, G.; Chavas, T. E. J.; Le Goff, X.; Gagosz, F. Biarylphosphonite Gold(I) Complexes as Superior Catalysts for Oxidative Cyclization of Propynyl Arenes into Indan-2-ones. *Angew. Chem., Int. Ed.* **2013**, *52*, 6277−6282.

(3) Zeng, X.; Soleilhavoup, M.; Bertrand, G. Gold-Catalyzed Intermolecular Markovnikov Hydroamination of Allenes with Secondary Amines. *Org. Lett.* **2009**, *11*, 3166−3169.
(4) Lavallo, V.; Frey, G. D.; Donnadieu, B.; Soleilhavoup, M.; Bertrand, G. Homogeneous Catalytic Hydroamination of Alkynes and Allenes with Ammonia. *Angew. Chem., Int. Ed.* **2008**, *47*, 5224−5228.
(5) Gaillard, S.; Bosson, J.; Ramón, R. S.; Nun, P.; Slawin, A. M. Z.; Nolan, S. P. Development of Versatile and Silver-Free Protocols for Gold(I) Catalysis. *Chem. - Eur. J.* **2010**, *16*, 13729−13740.
(6) Joost, M.; Amgoune, A.; Bourissou, D. Reactivity of Gold Complexes towards Elementary Organometallic Reactions. *Angew. Chem., Int. Ed.* **2015**, *54*, 15022−15045.
(7) Wang, J.; Lv, S.; Chen, H.; Shi, M.; Zhang, J. Isolation and characterization of gem-diaurated species having two C-Au σ bonds in gold(I)-activated amidiniumation of alkynes. *Dalton Trans.* **2016**, *45*, 17091−17094.
(8) Hashmi, A. S. K.; Lauterbach, T.; Nösel, P.; Vilhelmsen, M. H.; Rudolph, M.; Rominger, F. Dual Gold Catalysis: sigma, pi-Propyne Acetylide and Hydroxyl-Bridged Digold Complexes as Easy-to-prepare and Easy-to-handle Pre-Catalysts. *Chem. - Eur. J.* **2013**, *19*, 1058−1065.
(9) Lauterbach, T.; Asiri, A. M.; Hashmi, A. S. K. Organometallic Intermediates of Gold Catalysis. *Adv. Organomet. Chem.* **2014**, *62*, 261−297.
(10) Li, D.; Che, C.-M.; Kwong, H.-L.; Yam, V.W.-W. Photoinduced C-C bond formation from alkyl halides catalysed by luminescent dinuclear gold(I) and copper(I) complexes. *J. Chem. Soc., Dalton Trans.* **1992**, 3325−3329.
(11) Gasparrini, F.; Giovannoli, M.; Misiti, D.; Natile, G.; Palmieri, G.; Maresca, L. Gold(III)-catalyzed one-pot synthesis of isoxazoles from terminal alkynes and nitric acid. *J. Am. Chem. Soc.* **1993**, *115*, 4401−4402.
(12) Hashmi, A. S. K.; Schwarz, L.; Choi, J.-H.; Frost, T. M. A New Gold-Catalyzed C-C-Bond Formation. *Angew. Chem., Int. Ed.* **2000**, *39*, 2285−2288.
(13) Hashmi, A. S. K.; Frost, T. M.; Bats, J. W. Highly Selective Gold-Catalyzed Arene Synthesis. *J. Am. Chem. Soc.* **2000**, *122*, 11553−11554.
(14) Cheong, P. H.-Y.; Morganelli, P.; Luzung, M. R.; Houk, K. N.; Toste, F. D. Gold-Catalyzed Cycloisomerization of 1,5-Allenynes via Dual Activation of an Ene Reaction. *J. Am. Chem. Soc.* **2008**, *130*, 4517−4526.
(15) Weber, D.; Tarselli, M. A.; Gagné, M. R. Mechanistic Surprises in the Gold(I)-Catalyzed Intramolecular Hydroarylation of Allenes. *Angew. Chem., Int. Ed.* **2009**, *48*, 5733−5736.
(16) Levin, M. D.; Toste, F. D. Gold-Catalyzed Allylation of Aryl Boronic Acids: Accessing Cross-Coupling Reactivity with Gold. *Angew. Chem., Int. Ed.* **2014**, *53*, 6211−6215.
(17) Wolf, W. J.; Winston, M. S.; Toste, F. D. Exceptionally Fast Carbon-Carbon Bond Reductive Elimination from Gold(III). *Nat. Chem.* **2014**, *6*, 159−164.
(18) Komiya, S.; Kochi, J. K. Electrophilic cleavage of organogold complexes with acids. The mechanism of the reductive elimination of dialkyl(aniono)gold(III) species. *J. Am. Chem. Soc.* **1976**, *98*, 7599−7607.
(19) Rao, W.; Koh, M. J.; Li, D.; Hirao, H.; Chan, P. W. H. Gold-Catalyzed Cycloisomerization of 1,6-Diyne Carbonates and Esters to 2,4a-Dihydro-1*H*-fluorenes. *J. Am. Chem. Soc.* **2013**, *135*, 7926−7932.
(20) Grirrane, A.; Garcia, H.; Corma, A.; Álvarez, E. Air-stable, dinuclear and tetranuclear σ,π-acetylide gold(I) complexes and their catalytic implications. *Chem. - Eur. J.* **2013**, *19*, 12239−12244.
(21) Hashiguchi, B. G.; Bischof, S. M.; Konnick, M. M.; Periana, R. A. Designing Catalysts for Functionalization of Unactivated C-H Bonds Based on the CH Activation Reaction. *Acc. Chem. Res.* **2012**, *45*, 885−898.
(22) Jones, C. J.; Taube, D.; Ziatdinov, V. R.; Periana, R. A.; Nielsen, R. J.; Oxgaard, J.; Goddard, W. A., III Selective Oxidation of Methane to Methanol Catalyzed, with C-H Activation, by Homogeneous, Cationic Gold. *Angew. Chem., Int. Ed.* **2004**, *43*, 4626−4629.
(23) Lu, P.; Boorman, T. C.; Slawin, A. M. Z.; Larrosa, I. Gold(I)-Mediated C-H Activation of Arenes. *J. Am. Chem. Soc.* **2010**, *132*, 5580−5581.
(24) Boorman, T. C.; Larrosa, I. Gold-mediated C-H bond functionalization. *Chem. Soc. Rev.* **2011**, *40*, 1910−1925.
(25) Zavyalova, U.; Holena, M.; Schlögl, R.; Baerns, M. Statistical Analysis of Past Catalytic Data on Oxidative Methane Coupling for New Insights into the Composition of High-Performance Catalysts. *ChemCatChem* **2011**, *3*, 1935−1947.
(26) Farrell, B. L.; Igenegbai, V. O.; Linic, S. A Viewpoint on Direct Methane Conversion to Ethane and Ethylene Using Oxidative Coupling on Solid Catalysts. *ACS Catal.* **2016**, *6*, 4340−4346.
(27) Bayrakdar, T. A. C. A.; Scattolin, T.; Maa, X.; Nolan, S. P. Dinuclear gold(i) complexes: from bonding to applications. *Chem. Soc. Rev.* **2020**, *49*, 7044−7100.
(28) Paul, A. M.; Bent, B. E. Alkyl Coupling on Copper, Silver, and Gold: Correlation Between the Coupling Rate and the Metal-Alkyl Bond Strength. *J. Catal.* **1994**, *147*, 264−271.
(29) Komiya, S.; Albright, T. A.; Hoffmann, R.; Kochi, J. K. Reductive Elimination and Isomerization of Organogold complexes. Theoretical Studies of Trialkylgold Species as Reactive Intermediates. *J. Am. Chem. Soc.* **1976**, *98*, 7255−7265.
(30) Lawrence Kuch, P.; Stuart Tobias, R. Synthesis of cationic dialkylgold(III) complexes: nature of the facile reductive elimination of alkane. *J. Organomet. Chem.* **1976**, *122*, 429−446.
(31) Kochi, J. K. Electron-transfer mechanisms for organometallic intermediates in catalytic reactions. *Acc. Chem. Res.* **1974**, *7*, 351−360.
(32) Tamaki, A.; Kochi, J. K. Formation and decomposition of alkylgold(I) complexes. *J. Organomet. Chem.* **1973**, *61*, 441−450.
(33) Xu, H.; Diccianni, J. B.; Katigbak, J.; Hu, C.; Zhang, Y.; Diao, T. Bimetallic C-C Bond-Forming Reductive Elimination from Nickel. *J. Am. Chem. Soc.* **2016**, *138*, 4779−4786.
(34) Goj, L. A.; Blue, E. D.; Delp, S. A.; Gunnoe, T. B.; Cundari, T. R.; Petersen, J. L. Single-Electron Oxidation of Monomeric Copper(I) Alkyl Complexes: Evidence for Reductive Elimination through Bimolecular Formation of Alkanes. *Organometallics* **2006**, *25*, 4097−4104.
(35) Lail, M.; Gunnoe, T. B.; Barakat, K. A.; Cundari, T. R. Conversions of Ruthenium(III) Alkyl Complexes to Ruthenium(II) through Ru-C_{alkyl} Bond Homolysis. *Organometallics* **2005**, *24*, 1301−1305.
(36) Johnson, M. T.; Marthinus Janse van Rensburg, J.; Axelsson, M.; Ahlquist, M. S. G.; Wendt, O. F. Reactivity of NHC Au(I)-C σ-bonds with electrophiles. An investigation of their possible involvement in catalytic C-C bond formation. *Chem. Sci.* **2011**, *2*, 2373−2377.
(37) Yang, Y.; Eberle, L.; Mulks, F. F.; Wunsch, J. F.; Zimmer, M.; Rominger, F.; Rudolph, M.; Hashmi, A. S. K. Trans Influence of Ligands on the Oxidation of Gold(I) Complexes. *J. Am. Chem. Soc.* **2019**, *141*, 17414−17420.
(38) Yang, Y.; Schießl, J.; Zallouz, S.; Göker, V.; Gross, J.; Rudolph, M.; Rominger, F.; Hashmi, A. S. K. Gold-Catalyzed sp2-sp C-C Coupling by Alkynylation via Oxidative Addition of Bromoalkynes. *Chem. - Eur. J.* **2019**, *25*, 9624−9628.
(39) Hashmi, A. S. K.; Ramamurthi, T. D.; Rominger, F. Synthesis, Structure and Reactivity of Organogold Compounds of Relevance to Homogeneous Gold Catalysis. *J. Organomet. Chem.* **2009**, *694*, 592−597.
(40) Cui, L.; Zhang, G.; Zhang, L. Homogeneous gold-catalyzed efficient oxidative dimerization of propargylic acetates. *Bioorg. Med. Chem. Lett.* **2009**, *19*, 3884−3887.
(41) Zhang, G.; Cui, L.; Wang, Y.; Zhang, L. Homogeneous Gold-Catalyzed Oxidative Carboheterofunctionalization of Alkenes. *J. Am. Chem. Soc.* **2010**, *132*, 1474−1475.
(42) Hashmi, A. S. K.; Ramamurthi, T. D.; Todd, M. H.; Tsang, A. S. K.; Graf, K. Gold-Catalysis: Reactions of Organogold Compounds with Electrophiles. *Aust. J. Chem.* **2010**, *63*, 1619−1626.
(43) Vikse, K. L.; Zavras, A.; Thomas, T. H.; Ariafard, A.; Khairallah, G. N.; Canty, A. J.; Yates, B. F.; O'Hair, R. A. J. Prying open a

https://dx.doi.org/10.1021/jacs.0c11296
J. Am. Chem. Soc. 2021, 143, 2509−2522

Reactive Site for Allylic Arylation by Phosphine-Ligated Geminally Diaurated Aryl Complexes. *Organometallics* **2015**, *34*, 3255−3263.
(44) Seidel, G.; Lehmann, C. W.; Fürstner, A. Elementary Steps in Gold Catalysis: The Significance of gem-Diauration. *Angew. Chem., Int. Ed.* **2010**, *49*, 8466−8470.
(45) Gómez-Suárez, A.; Dupuy, S.; Slawin, A. M. Z.; Nolan, S. P. Straightforward Synthetic Access to gem-Diaurated and Digold σ,π-Acetylide Species. *Angew. Chem., Int. Ed.* **2013**, *52*, 938−942.
(46) Espada, M. F.; Campos, J.; López-Serrano, J.; Poveda, M. L.; Carmona, E. Methyl-, Ethenyl-, and Ethynyl-Bridged Cationic Digold Complexes Stabilized by Coordination to a Bulky Terphenylphosphine Ligand. *Angew. Chem., Int. Ed.* **2015**, *54*, 15379−15384.
(47) A convenient alternative method towards the Au-hydrocarbyl complex based on boronic acids appeared during the preparation of this manuscript: Tzouras, N. V.; Saab, M.; Janssens, W.; Cauwenbergh, T.; Hecke, K. V.; Nahra, F.; Nolan, S. P. Simple Synthetic Routes to N-Heterocyclic Carbene Gold(I)-Aryl Complexes: Expanded Scope and Reactivity. *Chem. - Eur. J.* **2020**, *26*, 5541−5551.
(48) Pérez-Galán, P.; Delpont, N.; Herrero-Gómez, E.; Maseras, F.; Echavarren, A. M. Metal-Arene Interactions in Dialkylbiarylphosphane Complexes of Copper, Silver, and Gold. *Chem. - Eur. J.* **2010**, *16*, 5324−5332.
(49) Ni, Q.-L.; Jiang, X.-F.; Huang, T.-H.; Wang, X.-J.; Gui, L.-C.; Yang, K.-G. Gold(I) Chloride Complexes of Polyphosphine Ligands with Electron-Rich Arene Spacer: Gold-Arene Interactions. *Organometallics* **2012**, *31*, 2343−2348.
(50) Caracelli, I.; Zukerman-Schpector, J.; Tiekink, E. R. T. Supramolecular synthons based on gold···π(arene) interactions. *Gold Bull.* **2013**, *46*, 81−89.
(51) Zuccarello, G.; Zanini, M.; Echavarren, A. M. Buchwald-Type Ligands on Gold(I) Catalysis. *Isr. J. Chem.* **2020**, *60*, 360−372.
(52) Marín, M.; Moreno, J. J.; Navarro-Gilabert, C.; Álvarez, E.; Maya, C.; Peloso, R.; Nicasio, M. C.; Carmona, E. Synthesis, Structure and Nickel Carbonyl Complexes of Dialkylterphenyl Phosphines. *Chem. - Eur. J.* **2019**, *25*, 260−272.
(53) Li, G.; Liu, C.; Lei, Y.; Jin, R. Au_{25} nanocluster-catalyzed Ullmann-type homocoupling reaction of aryl iodides. *Chem. Commun.* **2012**, *48*, 12005−12007.
(54) Li, G.; Abroshan, H.; Liu, C.; Zhuo, S.; Li, Z.; Xie, Y.; Kim, H. J.; Rosi, N. L.; Jin, R. Tailoring the Electronic and Catalytic Properties of Au_{25} Nanoclusters via Ligand Engineering. *ACS Nano* **2016**, *10*, 7998−8005.
(55) Vilhanová, B.; Václavík, J.; Artiglia, L.; Ranocchiari, M.; Togni, A.; van Bokhoven, J. A. Subnanometer Gold Clusters on Amino-Functionalized Silica: An Efficient Catalyst for the Synthesis of 1,3-Diynes by Oxidative Alkyne Coupling. *ACS Catal.* **2017**, *7*, 3414−3418.
(56) Cher, M. The Reaction of Methyl Radicals with Toluene. *J. Phys. Chem.* **1964**, *68*, 1316−1321.
(57) Schmidbaur, H.; Schier, A. A briefing on aurophilicity. *Chem. Soc. Rev.* **2008**, *37*, 1931−1951.
(58) Schmidbaur, H.; Schier, A. Aurophilic interactions as a subject of current research: an up-date. *Chem. Soc. Rev.* **2012**, *41*, 370−412.
(59) Weber, D.; Jones, T. D.; Adduci, L. L.; Gagné, M. R. Strong Electronic and Counterion Effects on Geminal Digold Formation and Reactivity as Revealed by Gold(I)-Aryl Model Complexes. *Angew. Chem., Int. Ed.* **2012**, *51*, 2452−2456.
(60) Adams, R. D.; Luo, Z.; Chen, M.; Rassolov, V. Multicenter transformations of the methyl ligand in CH_3Os_3Au carbonyl cluster complexes: Synthesis, characterization and DFT analyses. *J. Organomet. Chem.* **2016**, *812*, 95−107.
(61) Campos, J. Dihydrogen and Acetylene Activation by a Gold(I)/Platinum(0) Transition Metal Only Frustrated Lewis Pair. *J. Am. Chem. Soc.* **2017**, *139*, 2944−2947.
(62) Hidalgo, N.; Moreno, J. J.; Pérez-Jiménez, M.; Maya, C.; López-Serrano, J.; Campos, J. Evidence for Genuine Bimetallic Frustrated Lewis Pair Activation of Dihydrogen with Gold(I)/Platinum(0) Systems. *Chem. - Eur. J.* **2020**, *26*, 5982−5993.
(63) Schulz, J.; Shcherbachenko, E.; Roithová, J. Investigation of Geminally Diaurated Arene Complexes in the Gas Phase. *Organometallics* **2015**, *34*, 3979−3987.
(64) Adams, R. D.; Luo, Z. High nuclearity clusters containing methyl groups. Synthesis and structures of pentaosmium-gold carbonyl cluster compounds. *J. Organomet. Chem.* **2016**, *812*, 108−114.
(65) Campos, J. Bimetallic cooperation across the periodic table. *Nat. Rev. Chem.* **2020**, *4*, 696−702.
(66) Buchwalter, P.; Rosé, J.; Braunstein, P. Multimetallic Catalysis Based on Heterometallic Complexes and Clusters. *Chem. Rev.* **2015**, *115*, 28−126.
(67) Farley, C. M.; Uyeda, C. Organic Reactions Enabled by Catalytically Active Metal-Metal Bonds. *Trends Chem.* **2019**, *1*, 497−509.
(68) Ortega-Moreno, L.; Fernández-Espada, M.; Moreno, J. J.; Navarro-Gilabert, C.; Campos, J.; Conejero, S.; López-Serrano, J.; Maya, C.; Peloso, R.; Carmona, E. Synthesis, properties, and some rhodium, iridium, and platinum complexes of a series of bulky m-terphenylphosphine ligands. *Polyhedron* **2016**, *116*, 170−181.
(69) Uson, R.; Laguna, A.; Laguna, M.; Briggs, D. A.; Murray, H. H.; Fackler, J. P., Jr (Tetrahydrothiophene)Gold(I) or Gold(III) Complexes. *Inorg. Synth.* **2007**, *26*, 85−91.
(70) Hashmi, A. S. K.; Rudolph, M.; Huck, J.; Frey, W.; Bats, J. W.; Hamzić, M. Gold Catalysis: Switching the Pathway of the Furan-Yne Cyclization. *Angew. Chem., Int. Ed.* **2009**, *48*, 5848−5852.
(71) Mézailles, N.; Ricard, L.; Gagosz, F. Phosphine Gold(I) Bis(trifluoromethanesulfonyl)imidate Complexes as New Highly Efficient and Air-Stable Catalysts for the Cycloisomerization of Enynes. *Org. Lett.* **2005**, *7*, 4133−4136.
(72) Ho, T.-L.; Fieser, M.; Fieser, L. Gold(I) Nitrate - Triphenylphosphine. In *Fieser and Fieser's Reagents for Organic Synthesi*; Fieser, L. F., Fieser, M., Ho, T.-L., Eds.; John Wiley & Sons, 2011. DOI: 10.1002/9780471264194.fos11741.
(73) Mueting, A. M.; Alexander, B. D.; Boyle, P. D.; Casalnuovo, A. L; Ito, L. N.; Johnson, B. J.; Pignolet, L. H.; Leeaphon, M.; Meyer, K. E.; Walton, R. A.; Heinekey, D. M.; Harper, T. G. P. Mixed-Metal-Gold Phosphine Cluster Compounds. In *Inorganic Syntheses*; Grimes, R.N., Ed.; John Wiley & Sons, 1992. DOI: 10.1002/9780470132609.ch63.
(74) Nieto-Oberhuber, C.; López, S.; Echavarren, A. M. Intramolecular [4 + 2] Cycloadditions of 1,3-Enynes or Arylalkynes with Alkenes with Highly Reactive Cationic Phosphine Au(I) Complexes. *J. Am. Chem. Soc.* **2005**, *127*, 6178−6179.
(75) Wang, Y.; Ji, K.; Lan, S.; Zhang, L. Rapid Access to Chroman-3-Ones via Gold-Catalyzed Oxidation of Propargyl Aryl Ethers. *Angew. Chem., Int. Ed.* **2012**, *51*, 1915−1918.
(76) Sánchez-Cantalejo, F.; Priest, J. D.; Davies, P. W. A Gold Carbene Manifold to Prepare Fused γ-Lactams by Oxidative Cyclisation of Ynamides. *Chem. - Eur. J.* **2018**, *24*, 17215−17219.
(77) Zhdanko, A.; Ströbele, M.; Maier, M. E. Coordination Chemistry of Gold Catalysts in Solution: A Detailed NMR Study. *Chem. - Eur. J.* **2012**, *18*, 14732−14744.
(78) Fehr, C.; Vuagnoux, M.; Buzas, A.; Arpagaus, J.; Sommer, H. Gold- and Copper-Catalyzed Cycloisomerizations towards the Synthesis of Thujopsanone-Like Compounds. *Chem. - Eur. J.* **2011**, *17*, 6214−6220.
(79) Alférez, M. G.; Moreno, J. J.; Hidalgo, N.; Campos, J. Reversible Hydride Migration from C_5Me_5 to Rh^I Revealed by a Cooperative Bimetallic Approach. *Angew. Chem., Int. Ed.* **2020**, *59*, 20863−20867.
(80) Han, Z.-Y.; Guo, R.; Wang, P.-S.; Chen, D.-F.; Xiao, H.; Gong, L.-Z. Enantioselective concomitant creation of vicinal quaternary stereogenic centers via cyclization of alkynols triggered addition of azlactones. *Tetrahedron Lett.* **2011**, *52*, 5963−5967.
(81) Mayo, D. W.; Bellamy, L. J.; Merklin, G. T.; Hannah, R. W. The application of resolution enhancement techniques to the study of factors affecting group frequencies-I. Coupling of symmetric methyl

https://dx.doi.org/10.1021/jacs.0c11296
J. Am. Chem. Soc. 2021, 143, 2509−2522

deformation frequencies in o-xylene. *Spectrochim. Acta* **1985**, *41*, 355−357.

https://dx.doi.org/10.1021/jacs.0c11296
J. Am. Chem. Soc. 2021, 143, 2509−2522